THESIS FOR THE DEGREE OF DOCTOR OF PHILOSOPHY

Gas-filled, flat plate solar collectors

Johan Vestlund

Building Services Engineering
Department of Energy and Environment
Chalmers University of Technology
Gothenburg, Sweden, 2012

Gas-filled, flat plate solar collectors

JOHAN VESTLUND

ISBN 978-91-7385-621-8

Doktorsavhandlingar vid Chalmers tekniska högskola,
Ny serie nr 3302
ISSN 0346-718X

Technical report D2012:02
Building Services Engineering
Department of Energy and Environment
Chalmers University of Technology
SE-412 96 GÖTEBORG
Sweden
Telephone:+46 (0)31 772 1000

Printed by
Chalmers Reproservice
Göteborg 2012

Gas-filled, flat plate solar collectors

JOHAN VESTLUND
Building Services Engineering, Department of Energy and Environment
Chalmers University of Technology

Abstract

This work treats the thermal and mechanical performances of gas-filled, flat plate solar collectors in order to achieve a better performance than that of air filled collectors. The gases examined are argon, krypton and xenon which all have lower thermal conductivity than air. The absorber is formed as a tray connected to the glass. The pressure of the gas inside is near to the ambient and since the gas volume will vary as the temperature changes, there are potential risks for fatigue in the material.

One heat transfer model and one mechanical model were built. The mechanical model gave stresses and information on the movements. The factors of safety were calculated from the stresses, and the movements were used as input for the heat transfer model where the thermal performance was calculated.

It is shown that gas-filled, flat plate solar collectors can be designed to achieve good thermal performance at a competitive cost. The best yield is achieved with a xenon gas filling together with a normal thick absorber, where normal thick means a 0.25 mm copper absorber. However, a great deal of energy is needed to produce the xenon gas, and if this aspect is taken into account, the krypton filling is better. Good thermal performance can also be achieved using less material; a collector with a 0.1 mm thick copper absorber and the third best gas, which is argon, still gives a better operating performance than a common, commercially produced, air filled collector with a 0.25 mm absorber.

When manufacturing gas-filled flat plate solar collectors, one way of decreasing the total material costs significantly, is by changing absorber material from copper to aluminium. Best yield per monetary outlay is given by a thin (0.3 mm) alu-minium absorber with an argon filling. A high factor of safety is achieved with thin absorbers, large absorber areas, rectangular constructions with long tubes and short distances between glass and absorber. The latter will also give a thin layer of gas which gives good thermal performance. The only doubt-

ful construction is an argon filled collector with a normal thick (> 0.50 mm) aluminium absorber.

In general, an assessment of the stresses for the proposed construction together with appropriate tests are recommended before manufacturing, since it is hard to predict the factor of safety; if one part is reinforced, some other parts can experience more stress and the factor of safety actually drops.

Keywords: Solar collectors, Modelling, Mechanical stresses, heated cavity, collector material

Svensk sammanfattning

Idén bakom detta projekt är att undersöka värmeprestanda för plana solfångare med innesluten ädelgasfyllning eftersom argon, krypton och xenon alla har lägre värmekonduktivitet än luft. Absorbatorn formas som ett tråg och ansluts till glaset; rummet däremellan fylls med någon av ädelgaserna. Eftersom temperatur varierar under drift kommer volymen variera, men konstruktionen är så mjuk att trycket förblir mer eller mindre konstant lika omgivningstryck. Volymvariationerna ger upphov till rörelser i konstruktionen vilka kan leda till utmattning i material varför även hållfasthetsmässiga undersökningar gjorts.

En termisk modell och en mekanisk modell byggdes. Den mekaniska modellen gav svar på spänningarnas storlek och hur lådan såg ut när gasvolymen ökade. Spänningarnas storlek kunde räknas om till säkerhetsfaktorer. Data om lådans deformation matades till den värmetekniska modellen varvid termisk prestanda räknades ut.

Det är lämpligt att använda följande mängder gas: [nl/m^2]: xenon 3,9, krypton 5,7 eller argon 8,6, där en nl (normalliter) menas gasvolymen vid 25 °C. Gasen ger solfångaren goda termiska prestanda även om absorbatorn görs mycket tunn; en gasfylld solfångare med 0,1 mm tjock kopparabsorbator har ungefär samma η_0 som en vanlig luftfylld med 0,25 mm. Vid högre driftstemperaturer minskar verkninsggraden på alla solfångare, men de gasfyllda minskar inte lika snabbt vilket tyder på lägre termiska förluster. För att minska på dyr koppar i konstruktionen går det även att tillverka absorbatorn i aluminium och erhålla samma termiska prestanda som hos helkopparalternativet. Hög säkerhetsfaktor erhålles med stor absorbatoryta, rektangulär konstruktion med långa rör och kort avstånd mellan absorbator och glas. När det senare kombineras med lämpliga gasmängder ger xenon högsta säkerhetsfaktorn, krypon därefter och sist argon. Det enda fallet med tveksam säkerhetsfaktor är kombinationen argon och tjock aluminiumabsorbator.

Val av gas och övrig konfiguration beror på intention med solfångaren. Maximalt levererad värmeenergi ger en xenonfylld med normaltjock absorbator; om hänsyn tas till energibehov vid produktion är dock krypton den som ger mest. Aluminium är billigare, men koppar lägre energibehov vid produktion. Mest utbyte för pengarna ger en relativt tunn aluminiumabsorbator ihop med argongas. Hållfasthetsberäkning med aktuella mått och en test rekommenderas dock före produktion.

Preface/Acknowledgements

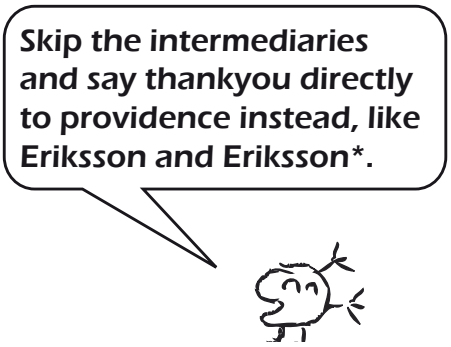

Unlike Eriksson and Eriksson* who said that they prefered to skip the intermediaries and thank providence directly, I am traditional and want to express my gratitude to all those concerned.

This work has been supported financially by The Knowledge Foundation in Sweden (KK-stiftelsen), Solentek AB and Högskolan Dalarna.

Many people have helped with the work over the years, either in the form of shared knowledge, discussions or reading of the manuscript. I would like to thank all of them and especially the following: Jan-Olof Dalenbäck, my supervisor from Chalmers University of Technology for good collaboration, accessibility and good spirits; Mats Rönnelid, assistant supervisor for useful feedback, instruction in the academic manner and initiating the project; Klaus Lorenz, company mentor for practical input and allowing the project to be carried out and finally Jill Gertzén, my language scrutinizer for assiduous work. Hopefully, I will be a scientist, but never an English teacher.

I would also like to thank everybody at the Solar Energy Research Center (SERC), Högskolan Dalarna, for creating and maintaining such a good and stimulating working environment. Lastly I would like to thank my wife Roos-Marie for putting up with my preoccupation during the work for a doctoral degree and my son Oscar for letting me use his cartoon figure in the doctoral work, and Mats for advice not to use this little man everywhere.

*Eriksson, R. and Eriksson, L., 2006. De norrbotniska satansverserna, ISBN: 978-91-7005-327-8, 133p.

Table of contents

1. INTRODUCTION

1.1 Solar energy and society

In 2008, the world energy demand was 518 EJ annually of which 81 % was extracted from fossil coal/peat, oil or gas. (IEA 2010)

There are reasons for replacing non-renewable energy with renewable. The almost never ending supply of renewable energy is one, and the precautionary principle another. IPCC (2007) reports that it is probable that there has been significant anthropogenic warming over the past 50 years, averaged over each continent (except Antarctica), mainly due to the emissions of greenhouse gases produced by coal, oil and gas. Therefore the precautionary reason for rejecting non-renewable energy sources would be a sufficient argument for increasing the renewable energy share. But obviously it is hard to reach agreement in questions like these; each local contribution is only marginal while it is the accumulated effects of actions that give a result. What makes it even more complicated is that there is a relation between GDP growth and growth in the consumption of oil which is usually called "business as usual". Business as usual makes the change from oil and other non renewable energy sources hard to motivate locally; policy makers, investors and end users therefore need to rethink and find other solutions not based on oil (Aleklett et al. 2010).

However, the supply sets the utmost limit and it is most critical for oil, where the global oil production has probably passed its peak (Aleklett et al. 2009).

One way of decreasing the use of fossil fuel is by increasing the efficiency of the energy used. The size of the potential can be discussed; a compilation done by Hammond (2004) showed that the thermodynamic (or exergetic) improvement potential is around 80%, but there is a technical barrier which limits the potential to about 50%, and economic barriers further reduce the potential to perhaps 30%. However, there still is a lot of energy which can be saved, with all barriers taken into account.

Thermal solar collectors can deliver heat for hot water systems and heated spaces and even cooling for cooled spaces. These two items stood for 23 and 86 EJ (exajoule) respectively in the worldwide figures for 2005 (Cullen and Allwood 2010a). If the sum of these two is the potential for thermal solar collectors, the total potential would be 109 EJ annually. In 2008, thermal solar energy contributed 0.49 EJ annually (SHC IEA 2010). This means that 99.5 %

of the solar collector market is still unexploited. Why exploitation is not higher cannot depend on the age of the invention; flat plate solar collectors with separate storage tanks were first developed by William J. Bailey in 1909 (Butti and Perlin 1980).

One possible reason why the thermal solar collector market is so little exploited is the crucial mass behaviour, described in the following. History is full of examples where new technologies replace older. Old systems are replaced with more effective systems, where system means some technological item or method. For example, the electromechanical calculator system was replaced by the electronic calculator system. Figure 1.1 shows how a system can be replaced by another. (Berg and Burvall 1998, Foster 1986)

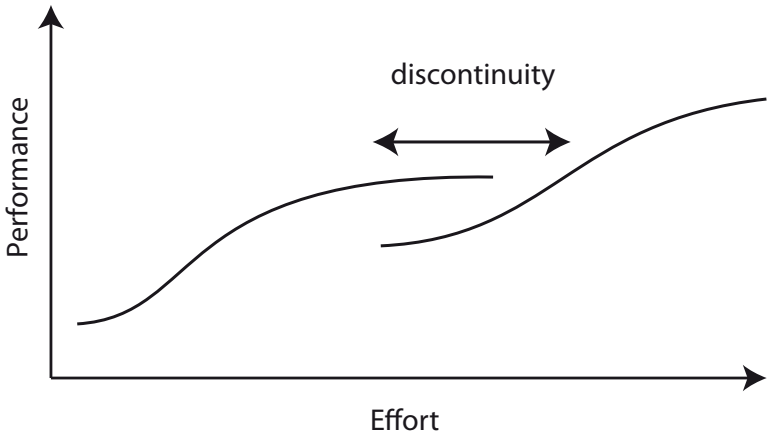

Figure 1.1 *S-curves. The performance of a technological system will be surpassed by a new system. Source Foster (1986)*

The S-curve gives an idea of the relation between the efforts that are carried out to increase the performance and the result achieved. To begin with the results from the efforts are poor, but when the required knowledge has been obtained, the performance increases fast, but the more money spent on developing the product, the harder it is to improve the technology. The sailing ship won't sail much faster, as Foster (1986) described the phenomenon.

If someone discovers or invents a new technology that has the potential of eventually become better than the existing system, the crucial part will be to bridge over the new system to give better performance than the old one. There are two possible ways of making this happen: Either by trusting the market forces; some entrepreneur sees a potential in a prospect and gets venture money,

develops the product and bridges over the discontinuity phase. The other way is with political instruments of control. The latter can be reduced to three different kinds: economical stimulation, regulations and information, or as Vedung (1988) also called them: Carrots, Sticks and Sermons. It is, however, not easy to open up a market with help of subsidies; there are many criteria that have to be fulfilled before an action like this can really be described as successful (Vedung 1998).

If the old S-curve, to the left in the figure, represents the non renewable systems of today, and the right hand S-curve represents some new system, a simple guess is that there will be several technology candidates for the right-hand curve. A crystal ball or maybe very initiated knowledge will be needed to know in advance which of them will dominate in the future. One of the candidates is solar heat, maybe combined with low energy buildings and seasonal heat storage and/or some extra heat source backup. With a market penetration of 0.5 % I dare to say that solar heat energy of today, generally, is in the discontinuity phase. It only depends on how the move is made from discontinuity to self evidence if Solar thermal is to gain a substantial share of the market for energy supply systems.

1.2 Thesis

1.2.1 Introduction

A factor of vital importance to allow thermal solar collectors to become self evident is the cost of producing such equipment. The price is dependent on material and assembly costs. The manufacturer can influence the assembly by rationalizing the production and it is a question of effort investments that can reduce the piece price. The material cost is more out of the manufacturer's control and it will be of interest to use less expensive material in the construction and to maximize the performance/price relation.

To sum up what has been said above, solar collector equipped systems in general need to be better for the customer compared to standard heat systems of today, otherwise the system replacement will never occur. Here, better means better totally, including low manufacturing costs, cheap energy during their lifetime, appearance, ease of installation, marginal maintenance, branding etc.

1.2.2 Gas-filled solar collectors

New efforts are continually being made to improve the performance and design of flat plate solar collectors. The more established designs now use proven manufacturing methods and offer reasonable but improvable performances.

The performance of a flat plate solar collector is, to a large extent, influenced by the thermal losses from the absorber to the ambient via the transparent cover. One way of reducing this heat loss is to reduce the convection by a transparent convection barrier such as a second glass or a plastic film. Another way is to reduce the thermal conductivity by using a more suitable gas than air. It is, of course, also possible to reduce this heat loss if the space between the absorber and the cover is evacuated. Double glazing implies an extra cost and weight, a plastic film requires an appropriate and durable mounting, a gas requires a sealed space, and evacuation implies a sealed space, as well as spacers, so the collector does not implode.

This study is focused on the design aspects of solar collectors with a sealed and gas-filled space between the glass cover and the absorber; aspects which have not previously been particularly well covered in literature.

Standard, commercially produced solar collectors have an air-filled cavity between the cover glass and the absorber. The aim of this work is to examine the feasibility of increasing the thermal performance of solar collectors by filling the cavity with a gas with more suitable, physical properties, for example, argon, krypton or xenon which all have lower thermal conductivity than air. Collectors with a noble gas filling are called gas-filled in the following chapters. Air is, of course, also a gas, but air-filled collectors are not included in the gas-filled collectors studied in this work.

Argon, krypton and xenon all have lower thermal conductivity than air and the idea behind this work is to examine if it is possible to produce solar collectors with a cavity filled with a gas with other, more suitable, physical properties, and thereby increase the thermal performance. Figure 1.2 shows a section of gas-filled collector.

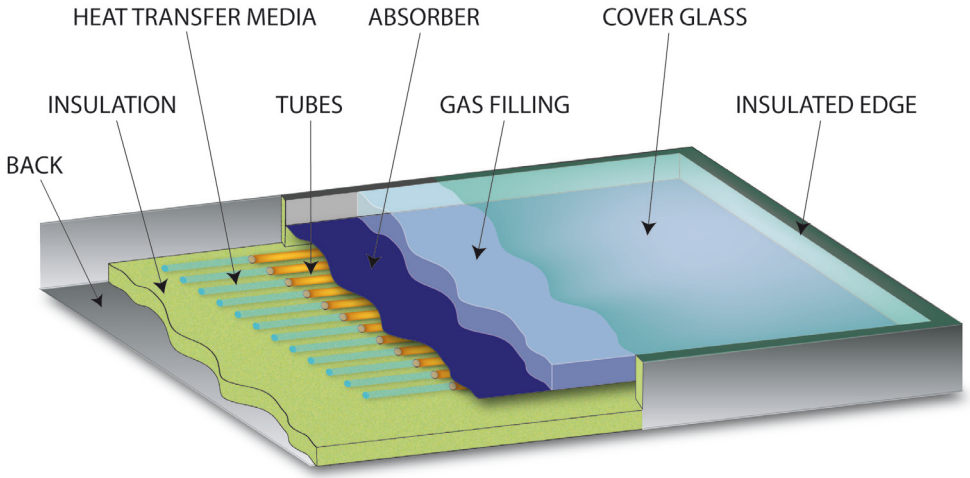

Figure 1.2 Section of a solar collector

The big difference between a gas-filled, flat plate solar collector and an air filled collector is that the cavity between the absorber and the cover glass is sealed and filled with a gas other than air. This has the following effects:

Firstly: Each gas has its own physical properties that affect the thermal performance, which will influence an assumed convection in the cavity. Therefore, how these physical properties affect the performance need to be examined.

Secondly: The solar collector box is not entirely stiff, but the amount which it can expand is not unlimited either. Therefore the gas will expand and contract depending on the temperature, at the same time as the pressure will also differ slightly. This may lead to potential risk for fatigue in material and this must also be checked.

Thirdly: there will be some side effects as well; for instance, there will be no dust or humidity on the inside of the glass or the absorber that can impair the performance.

1.2.3 Objectives

The objective is to study the design of gas-filled solar collectors from a thermal, as well as a mechanical, point of view. Compared with air, an inert gas reduces the heat loss, and a sealed space between the absorber and cover glass eliminates the influence of moisture and particles on the absorber.

However, a sealed space introduces volume and pressure variations during operation that, in turn, cause movements and mechanical stresses in the construction. This means that different design aspects will have to be considered when designing a gas filled, flat plate collector as opposed to an ordinary flat plate collector.

1.2.4 Method

The study is managed in three theoretical parts, supplemented with some experiments. First, the influence on thermal performance is studied using classic steady state heat balance theories involving conduction, convection and radiation. Second, the mechanical stress is studied using a finite element program. Third, the thermal performance and the mechanical stress are studied using an iterative procedure. Some basic measurements of a gas-filled solar collector have also been used to validate the calculations.

The study on thermal performance shows that it may be feasible to reduce the space between the absorber and the glass cover, and thereby the thickness of the collector, with maintained thermal performance. The study also indicates that the design of the absorber should be reconsidered in such a design. (Vestlund et al., 2009).

The study on mechanical stress shows that it is possible to reduce stress and improve the factor of safety by using a larger area and/or reducing the distance between the glass and the absorber and/or changing the length and width relationship of the absorber. (Vestlund et al., 2011a).

The combined effect of thermal performance and mechanical stress is then studied, based on the two previous studies, focusing more on the material in, and the design of, the absorber. (Vestlund et al., 2011b)

1.2.5 Limitations

The underlying reasons for the behaviour of the gases are not studied, since the reasons for their behaviour cannot be changed.

The gases studied were argon, krypton and xenon, with air as a reference. To be included in the study the gases had to fulfil certain conditions: they should have promising thermal properties, be toxic free, non corrosive, and free from other unwanted properties, such as a strong greenhouse effect, for example. Poor thermal properties excluded most of the gases; to begin with carbon dioxide was included, but it was not studied further since it was not more suitable than air. Sulphur hexafluoride (SF6) was not studied because of its strong greenhouse effect, even if the thermal properties are interesting.

The thermal calculations are based on conventional heat transfer relations for conduction, convection and radiation. Computational fluid dynamics (CFD) is not used.

Unsteady state heat transfer relation calculations are not studied since this is not particularly gas related.

The thermal loss in the connection between absorber and glass is not studied. Instead, the Tabor (1958) edge loss factor is used, which gives comparable values when changing one factor at the time, such as changing the gas and keeping the rest the same.

There is only one tube configuration i.e. a 12 mm tube laid in a meander pattern under the absorber. Some studies have been carried out on the thickness of tubes and variations of tube to tube distance, but parallel tubes or other configurations have not been studied since tube size and layout is not a gas specific problem.

The mechanical performance studies can give an approximate understanding of the stresses and factors of safety but they are not studied in great detail. There is a difference in the flexibility of the unit formed by absorber and tubes depending on whether different forces cause bending parallel to or perpendicular to the tube direction in the unit. The straight part of the tubes was included in the mechanical model since this has a large influence on the stresses, but the bends (in the meander layout) were not included since they have less influence: This allows the model to take into account the largest, most important forces

in one direction but not the full extent of the small, less important forces in the other direction, as shown in Figure 1.3.

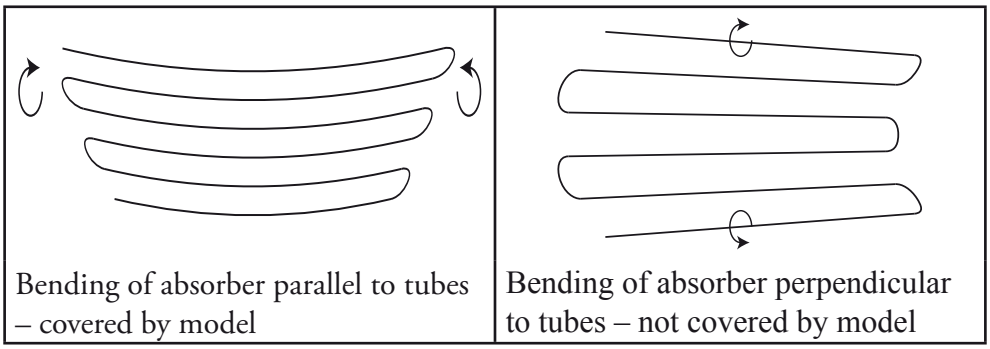

Figure 1.3 *The model takes the torsional moments along the tubes into account, while the smaller moments distributed in the bends of the tubes are not calculated*

Variations of connections between glass and absorber and the sealing are not studied in this work. There are already solar collectors filled with noble gases on the market, so these problems are rather a question of production technology than science, and are not particularly gas specific.

1.3 Articles

This thesis is based on three articles, described below.

I. Vestlund, J., M. Rönnelid and J-O. Dalenbäck (2009). Thermal Performance of Gas-filled Flat Plate Solar Collectors. Published (online Jan 24, 2009) in Solar Energy, Elsevier

II. Vestlund, J., Dalenbäck J-O. and Rönnelid M. (2011). Movement and mechanical stresses in sealed, flat plate solar Sol. Energy (2011), doi:10.1016/j.solener.2011.10.005, Elsevier

III. Vestlund, J., Dalenbäck J-O. and Rönnelid M. (2011). Thermal and mechanical performance of sealed, gas-filled, flat plate solar collectors. Sol. Energy (2011), doi:10.1016/j.solener.2011.08.023, Elsevier

The first article, focuses on thermal performance with no attention paid to thermal expansion of the hosted gas (i.e. an outer expansion vessel for the gas).

In the second article, stress and movement due to thermal expansion and contraction of the gas are analysed.

The third article describes the thermal as well as the mechanical performance of a gas-filled solar collector with attention paid to the expansion of the hosted gas. The effects of optimising the use of material is also analysed.

All research and all work in relation to the articles has been carried out by Vestlund. Co-authors Dalenbäck and Rönnelid are tutors and have been involved in discussions on the content and the result, and have reviewed and commented on the articles.

1.4 Outline

Article I focuses on the thermal performance of gas-filled flat plate solar collectors without movements due to changed temperature (i.e. there is a possibility for the gas to expand outside). Article II deals with the mechanical behaviour of a gas-filled flat plate solar collector where the gas expands and creates movements, i.e. absorber and glass are exposed to pressure variations. Article III combines the results from articles I and II. The thesis presents the topic in a more structured way.

Firstly, Chapter 2, SOLAR COLLECTOR THEORY, describes common solar collector theory. It includes non-gas specific formulas and theories required to understand the thermal behaviour of flat plate solar collectors.

Secondly, Chapter 3, MODELLING, describes the more specific relationships of gas-filled flat plate solar collectors based on modelling of thermal and mechanical performance. It also includes a part on model validation.

Thirdly, Chapter 4, RESULTS, presents the combined results concerning thermal and mechanical performance of gas-filled flat plate solar collectors. It also includes an evaluation of thermal collector yield, as well as production costs and energy requirements, for different designs of gas-filled flat plate solar collectors.

Fourthly, Chapter 5 DISCUSSION includes different aspects of the models used and assumptions made in the thesis and how some associated problems were solved. It also includes suggestions for future work.

Finally, Chapter 6, CONCLUSIONS, presents different aspects on configurations for, construction of and advantages with, gas-filled flat plate solar collectors.

2. SOLAR COLLECTOR THEORY

2.1 Performance and efficiency definition

There will be a difference between the usable power going out from the collector and the incoming solar irradiance. The difference between the irradiance and the usable power is called loss. This is described by Eq. 2.1.

$$q = A \bullet G_{Incident} - q_{Loss} \qquad \textit{Eq. 2.1}$$

where

q = Useful power [W]
A = Aperture area [m^2]
$G_{Incident}$ = Incident irradiance [W/m^2]
q_{Loss} = Loss power [W]

If the usable power going out from the collector is divided by the incoming irradiance power, the quotient describes the efficiency, as in Eq. 2.2.

$$\eta = \frac{q}{A \bullet G_{incident}} \qquad \textit{Eq. 2.2}$$

where

η = Efficiency [-]

2.2 Optical losses

There are several reasons for the loss. First, there will be an optical loss depending on the cover glazing; the solar beam passes the glass; most of the beam will pass through, but a small part will reflect from the glass. The quotient of what passes through and the incoming beam power is called transmittance (τ), and is defined in Eq. 2.3 (Duffie and Beckman 2006).

$$\tau = \frac{G_{t,c}}{G_{incident}} \qquad \textit{Eq. 2.3}$$

where

$G_{t,c}$ = Irradiance transmitted through the cover glass[W/m^2]

$G_{Incident}$ = Incident irradiance [W/m^2]

The beam that passes the glass will mainly be absorbed, but a small part of the beam will even be reflected back from the absorber and out again. The quotient of what is absorbed and what reaches the absorber is called admittance (α) and is defined in Eq. 2.4 (Duffie and Beckman, 2006).

$$\alpha = \frac{G_{Absorbed}}{G_{t,c}} \qquad \textit{Eq. 2.4}$$

where

$G_{Absorbed}$ = Absorbed irradiance [W/m^2]

There will be some optical losses when the light passes through the cover glass and when it is absorbed in the absorber. The ability to let the light through the glass is called transmittance (τ) and the ability to absorb the light is called asorbtance (α). Thus, the product formed by τα is the optical efficiency. Another factor worth mentioning is the incident angle modifier. The optical efficiency decreases the more the incident angle diverges from the normal to the glass, therefore it is necessary to take the impaired optical efficiency into account when calculating performance and this is done by an incidence angle modifier shown in Eq. 2.5 (Duffie and Beckman, 2006).

$$K_{\tau\alpha} = \frac{(\tau\alpha)}{(\tau\alpha)_n} \qquad \textit{Eq. 2.5}$$

where

$K_{\tau\alpha}$ = Incident angle modifier [-]

$(\tau\alpha)$ = optical efficiency at a certain incident angle [-]

$(\tau\alpha)_n$ = optical efficiency perpendicular to the collector [-]

Souka and Safwat (1966) found an incident angle modifier described in Eq. 2.6 can be used for flat plate solar collectors.

$$K_{\tau\alpha} = 1 + b_0\left(\frac{1}{\cos\theta} - 1\right) \qquad \textit{Eq. 2.6}$$

where

b_0 = incident angle modifier coefficient [-]

θ = angle between surface normal and incident radiation [rad or °]

In this study, the incident angle modifier is only used for yield calculations in the result, all other heat calculations assume irradiation perpendicular to the collector.

2.3 Thermal losses

There will be thermal losses which must be taken into account. When describing the actual heat loss at a certain temperature of the heat transfer media and at a certain ambient temperature, it is the temperature difference relation that is important; this is described by Eq. 2.7.

$$\Delta T = T_w - T_a \qquad \textit{Eq. 2.7}$$

where

ΔT = Difference between mean heat transfer media temperature and ambient temperature [K]

T_w = Mean temperature of heat transfer medium [°C]

T_a = ambient temperature [°C]

Cooper and Dunkle (1981) suggested a definition of the overall heat loss coefficient described in Eq. 2.8.

$$U_o = a + b(\Delta T) \qquad \textit{Eq. 2.8}$$

where

U_o = Heat loss coefficient referred to fluid temperature [W/(m^2, K)

a = Loss coefficient when mean temperature of heat transfer medium is the same as the ambient temperature [W/m^2, K]

b = Temperature dependant loss coefficient [W/(m^2, K^2)]

If the overall heat loss coefficient is analysed more thoroughly, it will be seen that there are several heat transfer relations forming this term. Many of this relations are nonlinear, so a substitution with a polynomial of first degree must therefore be an approximation, but the precision is better than it would be using a temperature independent U_o.

It would be convenient to describe the heat loss power as a product of $U_o \bullet \Delta T$, but attention must also be paid to losses depending on enhanced local temperatures on the absorber: Heat is also transported from each sun illuminated place on the absorber to the nearest tube. Therefore the absorber can also be seen as a fin where the heat is transferred to the nearest tube and further into the heat transfer media. In order for the desired heat transfer to occur, there must be a temperature difference between the absorber and the heat transfer media, and consequently the absorber must be warmer. The local temperature along the fin will vary when the solar collector is in use, and Figure 2.1 shows three typical examples of the temperatures along the fin for an ordinary, flat plate solar collector, at different temperature differences between heat transfer media and ambience.

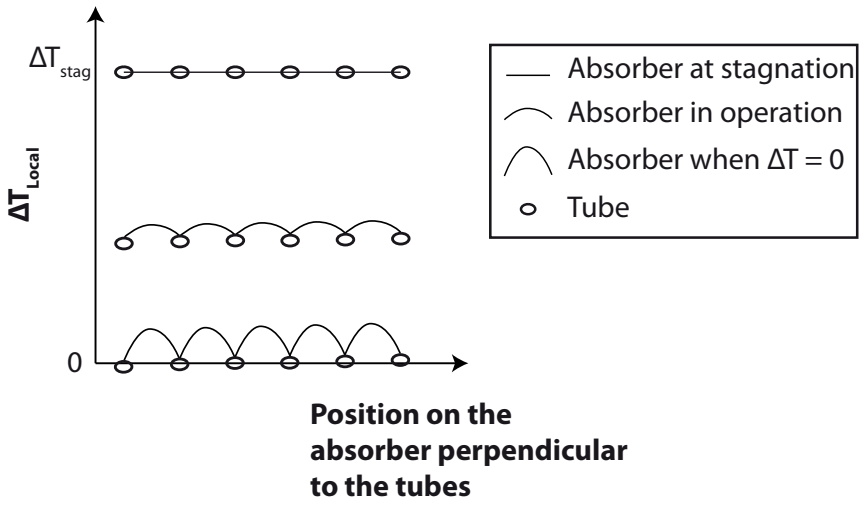

Figure 2.1 *Temperatures along the fin at different temperature differences between heat transfer media and ambient temperatures*

where

ΔT_{local} = Difference between each local point on fin and tube respectively and ambient temperature [K]

Some observations may be made here. Firstly: if the collector is in normal operation (the middle curve) and the heat transfer media temperature is decreased, the losses will decrease (described by Eq. 2.10 on page 16). This increases the heat transfer through the fin, which in its turn, leads to a greater temperature gradient along the fin, i.e. the lower the temperature in the heat transfer media the larger the temperature gradient on the fin. When the heat transfer media has the same temperature as the ambient temperature, the heat transfer is at its maximum and therefore the fin and the heat transfer media will have the largest temperature difference. On the other hand, if the heat transfer media temperature is increased, the losses (according to Eq. 2.10) will also increase, which reduces the heat transfer through the fin, which in its turn leads to a smaller temperature gradient along the fin at higher temperatures. If the heat transfer media temperature is further increased, at a certain temperature the losses will have the same magnitude as the incoming power. Therefore, there will be no heat transfer from the fin to the media and they will have the same temperature. This phenomenon is called stagnation.

The second observation is that the temperature gradient in the fin increases, in absolute terms, nearer the tube, which indicates that the heat transfer is largest nearest the tube. This can also be expected as the amount of power to be transported increases towards the tube. Unfortunately, the local enhanced temperature on the fin also leads to enhanced local losses. The greater the heat transported the larger the fall in temperature. This extra heat loss cannot be described by the product of $U_o \bullet \Delta T$, since the mean temperature of the heat transfer medium is not the same as the mean temperature of the absorber.

Since the fin dependant loss will affect the behaviour of the collector as soon as the mean fluid temperature and the ambient temperature are equal, it needs to be taken into account and is given a special term. This term is called fin efficiency, F', which is defined in Eq. 2.9 (Eisenmann 2002).

$$F' = \frac{q(\overline{T}_p)}{q(\overline{T}_p = \overline{T}_w)} \qquad \textit{Eq. 2.9}$$

where

q = Usable power [W]

T_p = Mean temperature of the absorber plate [°C]

T_w = Mean temperature of the heat transfer media [°C]

Eq. 2.9 defines F', but since it is difficult to determine Tp by measurement, F' cannot be calculated in this way and F' may be estimated using other formula. Since this work concentrates on the question of heat transfer, these formulas are omitted, but can be found in Eisenmann's dissertation (2002) written in German. There is also an article in English by Eisenmann et al. (2004).

For further equations, a definition is needed for the heat loss coefficient referring to mean plate temperature as in Eq. 2.10 (Cooper and Dunkle 1981).

$$U_l = \frac{U_o}{F'} \qquad \textit{Eq. 2.10}$$

where

U_l = Heat loss coefficient referred to mean plate temperature [W/(K,m^2)]

2.4 Power and efficiency

The usable power collected by the collector is described by Eq. 2.11 (Duffie and Beckman 2006).

$$q = F' \bullet A \bullet [\, (\tau \bullet \alpha) \bullet G - U_l \bullet \Delta T \,] \qquad \textit{Eq. 2.11}$$

If area and irradiation in Eq. 2.11 are rearranged, the efficiency can be described, as in Eq. 2.12.

$$\eta = F' \left[\tau \bullet \alpha - \frac{U_l \bullet \Delta T}{G} \right] \qquad \textit{Eq. 2.12}$$

$\Leftrightarrow$ (use the distributive law)

$$\eta = F' \ \tau \bullet \alpha - \frac{F' \bullet U_l \bullet \Delta T}{G} \qquad \textit{Eq. 2.13}$$

When $\Delta T = 0$, the term furthest to the right disappears in Eq. 2.13. The remaining part of the formula will describe the efficiency of the collector when the mean temperature of the heat transfer media is the same as the ambient. This is described in Eq. 2.14 (Cooper and Dunkle 1981).

$$\eta_0 = F' \bullet \tau \bullet \alpha \qquad \textit{Eq. 2.14}$$

where

η_0 = efficiency when mean temperature of heat transfer media is the same as the ambient [-].

When carrying out measurements on real collectors it is easier to determine η_0, and the terms a and b in Eq. 2.8. Therefore, Eq. 2.13 can be rewritten so it is easier to compare calculations and measurements. Eq. 2.17 is compiled by combining Eq. 2.8, Eq. 2.10 and Eq. 2.14.

Replace $F' \tau \bullet \alpha$ in Eq. 2.13 with η_0

$$\eta = \eta_0 - \frac{F' \bullet U_l \bullet \Delta T}{G} \qquad \textit{Eq. 2.15}$$

$\Leftrightarrow$

$$\eta = \eta_0 - \frac{U_o \bullet \Delta T}{G} \qquad \textit{Eq. 2.16}$$

$\Leftrightarrow$

$$\eta = \eta_0 - \frac{a\Delta T + b\Delta T^2}{G} \qquad \textit{Eq. 2.17}$$

With this formula it is possible to determine all terms by measurement.

Figure 2.2 shows the curve of the function $\eta(\Delta T)$, described by Eq. 2.17, with common values of η_0, a and b.

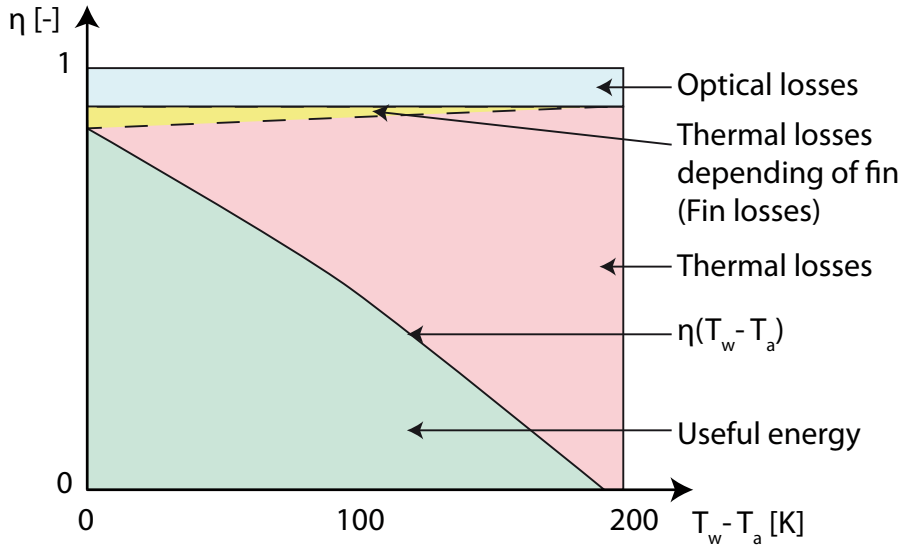

Figure 2.2 An efficiency curve for a normal, flat plate solar collector

The curve is based on a common, commercially produced, air filled, flat plate solar collector (values from reference 2), an ambient temperature of 25 °C and irradiation of 1000W/m^2.

The figure consists of different areas:

The optical loss; Temperature independent and therefore constant

The useful energy; is greatest when the heat transfer media temperature is equal to the ambient, but decreases as the difference increases.

The rest is thermal losses; where the upper part, over the dashed line (yellow), shows the loss due to raised local temperatures on the absorber depending on heat transfer, i.e. the fin losses, and the lower part (pink) shows the remaining losses.

It is notable that the reduction of efficiency at high temperatures mainly depends on the thermal losses described by the product of $U_o \bullet \Delta T$.

3. MODELLING

3.1 Thermal model

Thermal transfer can consist of conduction, convection and radiation. All formulas are not presented here, but for those who are interested in calculating the transfer rates in different situations, there are several books about heat transfer, such as Holman (2002), or Alvarez (1990).

A survey of why different gases in enclosed spaces differ in thermal performance follows. Radiation is, of course, also included in the total thermal transfer, but, as the distances are small, it will not differ from gas to gas and will not affect the result. Therefore it is omitted here.

3.1.1 Thermal transfer basics

Thermal transfer through a solid physical body can be calculated by taking the temperature difference, the conductivity and the shape factor into account, as in Figure 3.1.

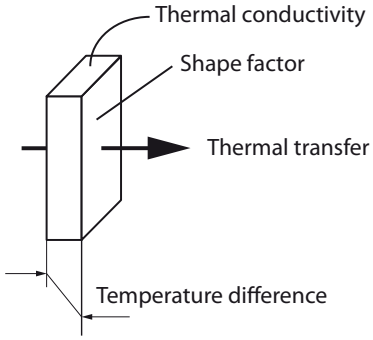

Figure 3.1 Thermal transfer by conduction

The formula is given in Eq. 3.18.

$$q_k = k\ S\ \Delta T \qquad \textit{Eq. 3.18}$$

where

q_k = Power of thermal conductance transfer [W]

k = Thermal conductivity; a material constant [W/(m^2,K)]

S = Shape factor [m]

ΔT = Temperature difference [K]

Conductance is the first material property presented here, which must be taken into account in the thermal performance calculation. When selecting materials, and a low thermal transfer is required, low conductance is preferable.

The shape factor describes how the physical dimensions of the body will affect the result. It is possible to calculate shape factors for different physical systems; there is, for example, a list of shape factors in Holman (2002). The factors to take into account for a body with a warm side and a cold side (such as a wall) are shown in Figure 3.2.

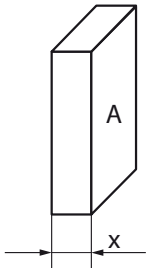

Figure 3.2 Shape factor for a wall is calculated on area and thickness

The heat transfer will be proportional to the area of the wall and in inverse proportion to the thickness of the wall and therefore the shape factor will be as described in Eq. 3.19.

$$S = \frac{A}{x} \qquad \textit{Eq. 3.19}$$

where

A = Area of the wall [m^2]

x = Thickness of the wall [m]

If the rigid body in the calculation is changed to a box with the same physical dimensions, and the cavity inside the box is filled with a gas, convection can occur, i.e. the gas can start to move around inside the box due to variations in density caused by temperature differences. These movements of the gas will

cause a larger heat transfer which must be taken into account. When calculating convection, the conduction formula, Eq. 3.18, can be adapted as shown in Eq. 3.20.

$$q_c = Nu\ k\ S\ \Delta T \qquad \textit{Eq. 3.20}$$

where

q_c = Power of thermal convection transfer [W]

Nu = Nusselts number [-]

The only new factor in the equation is the Nusselt number, abbreviated Nu, and this describes how much increased convection will amplify the heat transfer. Thus, Nu=1 means pure conduction and Nu > 1 means that convection and conduction occur at the same time.

For calculating convection within an enclosed, inclined cavity, which is the case with a gas filled solar collector, the Nusselt number will be dependant on two factors that are shown in Figure 3.3.

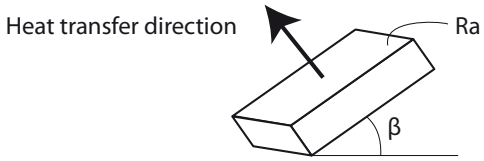

Figure 3.3 *The Nusselt number, which describes convection, is calculated on only two factors in an inclined box filled with a medium such as a gas*

The Nusselt number will be calculated as in Eq. 3.21 (Hollands et al. 1976).

$$Nu = 1 + 1.44\left[1 - \frac{1708(\sin 1.8\beta)^{1.6}}{Ra\cos\beta}\right]\left[1 - \frac{1708}{Ra\cos\beta}\right]^{+} + \left[\left(\frac{Ra\cos\beta}{5830}\right)^{1/3} - 1\right]^{+} \qquad \textit{Eq. 3.21}$$

where

β = Slope [rad or ° (= degrees)]

Ra = Rayleigh number [-]

+ exponent = Only positive values of the terms in the square brackets are to be used.

Eq. 3.21 is valid in a range for β between 15° and 60°. For larger angles, use equation described by EISherbiny et al. (1982).

The Rayleigh number (Ra) can be found by Eq. 3.22.

$$Ra = Gr\ Pr \qquad \textit{Eq. 3.22}$$

where

Gr = Grashof number [-]

Pr = Prandtl number [-]

The Prandtl number is the second material property which has to be taken into account for the thermal performance calculation in enclosed spaces filled with gas. When selecting a gas, and a low thermal transfer is wanted, a low Prandtl number is preferable.

The Grashof number is calculated as shown in Eq. 3.23.

$$Gr = \frac{g\ \rho\ \beta'\ \Delta T\ L^3}{\nu^2} \qquad \textit{Eq. 3.23}$$

where

g = Gravitational constant [9.81 m/s^2]

ρ = Density [kg/m^3]

β' = Volumetric constant of expansion, based on the mean temperature of the medium (β' = 1/T) [K-1]

ΔT = Temperature difference [K]

L = Plate spacing [m]

ν = Kinematic viscosity [m^2/s]

Density and kinematic viscosity are the third and the fourth material properties that have to be taken into account for the thermal performance calculation. If a low thermal transfer is wanted, the gas should preferably have a low density and a high kinematic viscosity.

As could be seen in the pure conduction calculation, (Eq. 3.20,) a long distance would be preferable for low thermal transfer, but for the convection, Eq. 3.23, shows that a short distance is preferable. Physically explained, this means that at short distances the heat transfer will be only by conduction, since the Grashof number will be low, and when the plate spacing increases, at some point convection starts, and this will increase thermal transfer.

3.1.2 Compilation of thermal transfer factors

The properties mentioned in section 3.1.1 are compiled in Table 3.1.

Table 3.1 Compilation of factors to take into account when calculating conduction and convection

Property	Lowering thermal transfer by	N.B.
Conductivity	Decrease	material property
Nusselt Number	Decrease	
Rayleigh number	Decrease	
Prandtl number	Decrease	material property
Grashof number	Decrease	
Density	Decrease	material property
Plate spacing	Increase (conduction) Decrease (convection)	
Viscosity	Increase	material property

The material properties that have some influence on the thermal performance for a gas are shown in Figure 3.4 which gives a brief description of the properties for air, argon, krypton and xenon within the operating temperature range for the collectors.

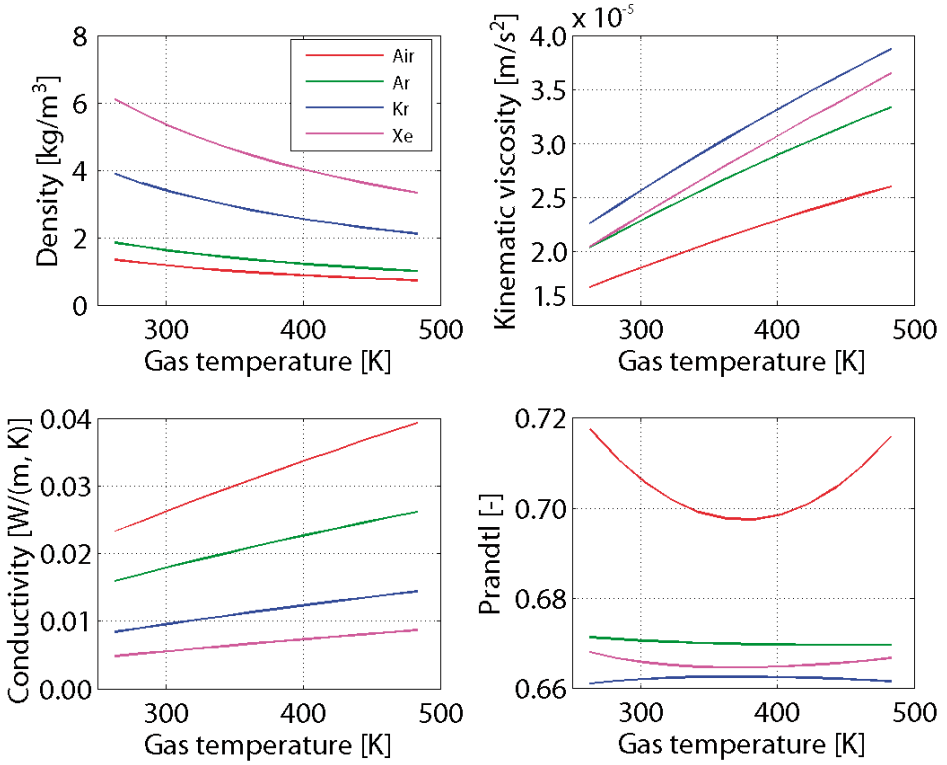

Figure 3.4 *Four material properties that influence heat transfer for four gases and their temperature dependencies*

material data comes from the measurement series Alvares (1990), Lide (1994), Holman (2002) and Air-Liquide (2006). The material data has been linearised when used in the collector model.

As can be seen in Figure 3.4, there is a significant difference between the conductivity for the gases. Given that there is no convection, xenon would be the most suitable gas followed by krypton, argon and finally air. For the properties which affect convection (i.e. Prandtl, density and kinematic viscosity) the density has the biggest variation and, inserted in the formulas, it is obvious that the succession order will be the reverse; air will have the lowest convection, followed by argon, krypton and xenon. This indicates that the same Nusselt number will occur for different distances between absorber and glass depending on the gas, where air will have the largest distance and xenon the smallest.

3.1.3 The setup of numerical methods for calculation

The solar collector model was calculated by numerical methods; that means, in principle, simple mathematics but many calculations. It is possible to calculate heat transfer by vectors and matrices, and in the following a brief explanation of the principles behind the calculations will be presented. This discussion does not aim to be complete; there are too many details – refer instead to standard literature on numerical methods. A book by Peter Pohl (1999) was used here.

An example of a simple heat transfer from a warmer to a colder position can be seen in Figure 3.5 and expressed in Eq. 3.24. The nomenclature is that warm and cold positions respectively are called nodes and the heat transfer media in between is called element.

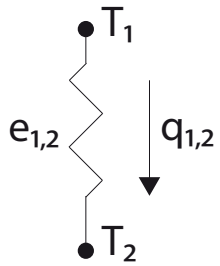

Figure 3.5 Heat transfer from position 1 to position 2.

$$q_{1,2} = e_{1,2}\,(T_1, T_2) \qquad \textit{Eq. 3.24}$$

where

$q_{1,2}$ = The heat transfer power from node 1 to 2 [W]
$e_{1,2}$ = The heat transfer element between node 1 and 2 [W/K]
T_1 = Temperature at node 1 [K]
T_2 = Temperature at node 2 [K]

Furthermore, a node can have more than one heat transfer element connection as in Figure 3.6, where node number 2 is studied with its neighbours 1, 3, 4 and 5.

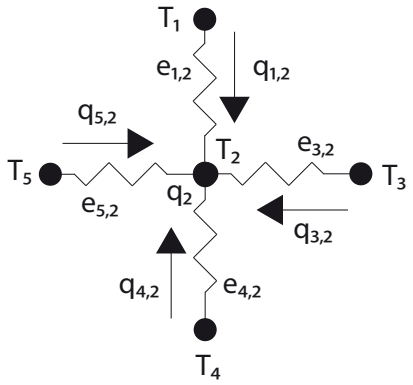

Figure 3.6 Heat transfer to one node is the sum all neighbouring nodes

As with Kirchhoff's laws in electricity, it is possible to count the sum of the heat transfers to a node, which is shown in Eq. 3.25.

$$q_2=e_{1,2}\,(T_1,T_2)+e_{3,2}\,(T_3,T_2)+e_{4,2}\,(T_4,T_2)+e_{5,2}\,(T_5,T_2) \qquad \textit{Eq. 3.25}$$

If heat transfer is taking place through node 2, one or more of the neighbouring nodes will be warmer than node 2 and one or more of the neighbours will be colder than the studied node. All the heat transfer into the node will be equal to the sum of all the heat transfer leaving the node. Since all heat transfer is added in equation 2, this means that the heat transfer leaving the node will have the opposite sign to the heat transfer into the node. To find the temperature of the node an assumption of the total heat transfer can be made. If the sum of the heat transfers is assumed to be 0, the temperature is established. But it is more likely that q2 will not be 0 and several other assumptions must be made.

Assume there are more nodes involved in the model and that more of the temperatures on the nodes are unknown; then there will be several equations such as Eq. 3.25. It is possible to form an equation system of all single equations as in Eq. 3.26:

$$\vec{q} = E\,\vec{T} \qquad \textit{Eq. 3.26}$$

where

$\vec{q}$ = A vector with the heat transfer sum at each node in the model; will be $\vec{0}$ when all temperatures are found.

E = A matrix consisting of all heat transfer relationships.

$\vec{T}$ = A vector with the temperature at each node in the model.

To find the temperatures, there are several methods available. When selecting a method, the criteria are: 1. Maximum deviation of the assumed temperature vector that is allowed initially and which still gives convergence of the system. 2: The time required to find the values of the temperature vector. Newton-Raphsson's method usually works well and is also time efficient. The method is described in Eq. 3.27, Eq. 3.28 and Eq. 3.29:

$$J = \frac{d\vec{q}}{d\vec{T_n}} \qquad \textit{Eq. 3.27}$$

$$\vec{t_n} = J^{-1} * \vec{q} \qquad \textit{Eq. 3.28}$$

$$\vec{T_{n+1}} = \vec{T_n} - \vec{t_n} \qquad \textit{Eq. 3.29}$$

where

n = Subscript that describes that this is an iterative process.

n+1 = Subscript referring to next iteration

J = A Jacobian matrix which describes how the different heat transfer sums change as the temperatures change.

$\vec{t_n}$ = Vector containing the temperature change for next try.

Eq. 3.26 to Eq. 3.29 is repeated until max($\vec{t_n}$) is so small that the truncate error is negligable.

3.1.4 The heat transfer matrix

As said earlier, the E matrix comprises all heat transfer relationships i.e. all small "e"s, as described in Eq. 3.24. An example of the function matrix is shown in Figure 3.7.

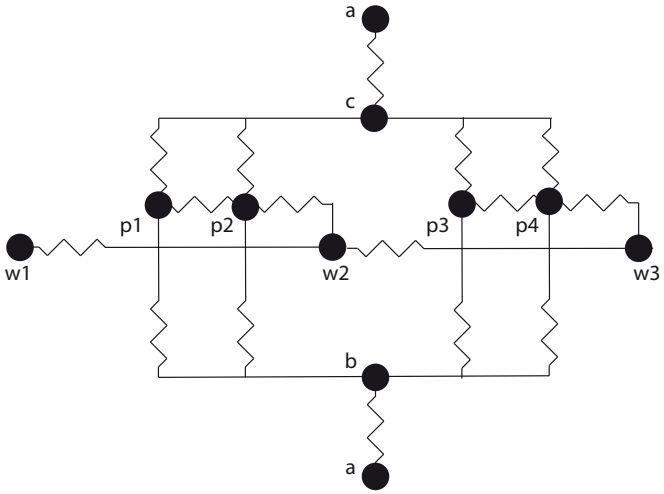

Figure 3.7 A simple solar collector model

In the collector example shown, the nodes are:

a = ambient air

b = Back

c = Cover glazing

p1 = Absorber plate; fin furthest away from tube, nearest incoming heat fluid

p2 = Absorber plate; fin nearest tube, nearest incoming heat fluid

p3 = Absorber plate; fin furthest away from tube, nearest outgoing heat fluid

p4 = Absorber plate; fin nearest tube, nearest outgoing heat fluid

w1 = Incoming heat fluid

w2 = Partly heated heat fluid

w3 = Outgoing heat fluid

The heat transfer elements also need some explanations:

$e_{b,a}$ = Heat losses from back to ambience; convection on inclined, open areas where the tilt angle < 0° + radiation to ambient air.

$e_{c,a}$ = Heat losses on front from cover glazing to ambience; convection on inclined, open areas where 0° < tilt angle < 90° + radiation to ambient air.

$e_{p,b}$ = Heat losses from absorber to back; Heat conduction.

$e_{p,c}$ Heat losses from absorber to cover glazing; convection in inclined, enclosed cavity taking into consideration area, tilt angle and distances including a calculation of how the distance is affected by the gas expansion/contraction depending on the mean temperature in the gas + radiation between absorber and glass.

$e_{p,p}$ = Heat transfer from one position on absorber to another; conduction in absorber plate with a distance between the nodes which is counted from centre to centre of the nodes.

$e_{p,w}$ = Heat transfer from absorber to the tube; conduction from absorber plate to the tube and a convection layer inside the tube.

$e_{w,w}$ = Temperature rise in the heat fluid; a rise of enthalpy of the incoming heat fluid corresponding to the temperatures at the two nodes. This function will only be used from colder to warmer nodes; the cold node nearer the inlet can never be heated by later alterations in the fluid heat.

The E matrix is then built up by placing the elements (the e's) in the correct position in the matrix. Actually, when a relation in the matrix is to be calculated, for example the relation between node 2 and 3, (e2,3) the algorithm checks the kind of relation between the nodes (ep,p, ep,w, ec,a etc), and then the calculation is performed with the correct formula. The relation of one node to another node in one direction is the same, but negative, in the other direction (e2,3 =-e3,2), so it will be calculated only once, but used twice, which will save time. Though, there is one exception and that is the ew,w relation, where a node is not affected by the next in the direction of flow.

3.1.5 The number of nodes

The resolution of the model also influences the result; the more nodes the better the precision. It is possible to vary the number of absorber nodes per tube node and the number of tube nodes. The reason for not greatly increasing the number of nodes is that the calculation time increases by the square of the number of nodes, since the matrix E is quadratic. Another reason is that the truncation error in the model gets smaller and smaller as more nodes are added,

but other errors that depend on other factors remain, and at some point the truncation error will be negligible in comparison. different sources of error are further discussed in 5.1.

3.1.6 Revisions of the model

The model has been refined during the work of the thesis. The most important improvements were:

1. The implementation of calculation with attention paid to the gas expansion/contraction (closed cavity functionality).

2. The rebuild for matrix calculation instead of double iteration loops - gave time-efficient calculation and higher precision due to more nodes and no more assumptions of temperature distribution.

3.2 Mechanical model

3.2.1 Introduction

A solar collector can be exposed to a large temperature range, and the upper and lower limits depend on the climate where the collector is to be used, but there will always be a range of temperatures. When enclosing a gas, the temperature will influence the volume and/or the pressure. Since the solar collector is assumed not to be equipped with an expansion vessel for the gas, and the collector will be made of soda-lime glass and metal, the construction has to handle these volumes and pressure variations.

The following sections will give a brief survey of important aspects of mechanical performance for gas filled solar collectors.

3.2.2 Relationship between stress and strain

To study a single axis example; if a rod is exposed to a tensile force at one end, there will be an equal but opposite force at the other end, as in Figure 3.8. This is described mathematically in Eq. 3.30.

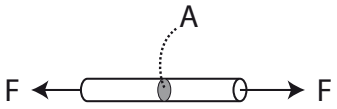

Figure 3.8 Force and area

$$-F + F = 0 \qquad \textit{Eq. 3.30}$$

where

F = Force [N]

The material of the rod will be exposed to a stress and that stress is defined in Eq. 3.31.

$$\sigma = \frac{F}{A} \qquad \textit{Eq. 3.31}$$

where

σ = Stress [N/m^2]

F = Force [N]

A = Cross section area [m^2]

The materials will then be deformed and that is illustrated by Figure 3.9.

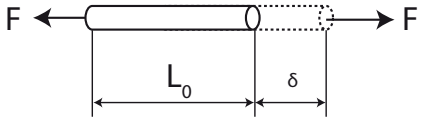

Figure 3.9 The force will elongate the rod

The elongation can be described as a strain if it is divided by the original length, as in Eq. 3.32

$$\varepsilon = \frac{\delta}{L_0} \qquad \textit{Eq. 3.32}$$

where

ε = Strain [-]

δ = Elongation [m]

L_0 = Original length [m]

There is a relationship between stress and strain. The more stress, the more strain, but the amount is dependant on the material. This material constant is called the elasticity modulus and is illustrated in Figure 3.10.

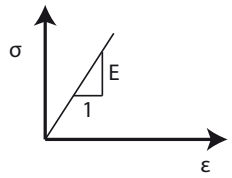

Figure 3.10 *The elasticity modulus describes the relation between stress and strain*

The relation between stress and strain is called Hookes law, and is described in Eq. 3.33.

$$\sigma = E\,\varepsilon \qquad \textit{Eq. 3.33}$$

where

σ = Stress [N/m^2, Pa]

E = Elastisity modulus [N/m^2, Pa]

ε = Strain [-]

3.2.3 Safeguard against fatigue

There is a limit to the size of the load a material can withstand. This limit is dependant on the size of the stresses in the material and if there are any kinds of variations in the load. The nomenclature used is given in Figure 3.11.

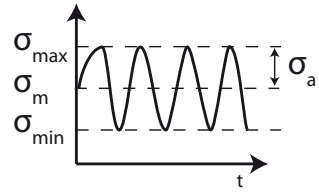

Figure 3.11 *Stress nomenclature with a varying load*

Assuming the construction will be subjected to very many stress cycles, the relation between the mean stress (σ_m) and the amplitude of the variation of the stress (σ_a) can be visualised in a Haigh diagram as in Figure 3.12.

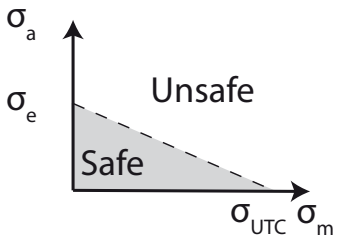

Figure 3.12 Haigh diagram with attention paid to persistence

There are some new definitions:

σ_e = Endurance: the limit of how much periodical stress the material can withstand repeated a number of times (typically 107 times).

σ_{UTC} = Ultimate strength: limit of how much stress the material can withstand when it is loaded once.

The safe area in the figure is limited by a straight line between the ultimate strength and the endurance limit.

One more limit is added to the Haigh diagram; deformation also needs to be taken into account. For a material such as steel, the material will recover its original shape completely up to a certain, small deformation level. But this is not the case when using copper or aluminium, because a small part of the deformation will always remain in these materials. The upper limit of persisting deformation is usually set to 0.2 %. The stress which causes a 0.2% deformation after the stress is released, is called "$\sigma_{p0.2}$" and is added in the Haigh diagram, shown in Figure 3.13.

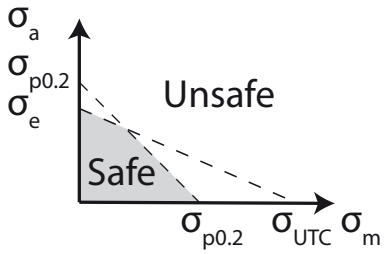

Figure 3.13 Haigh diagram with attention paid to persistence and deformation

As can be seen in the diagram, the safe area is now limited by two lines, and, depending on material, the exhaustion, ultimate strength and persistence stress limits will vary, which means that the persistence stress limit may be larger than one or both of the other limits.

If the stress mean and amplitude is known, it is possible to define a working point (a dot in the Haigh diagram) for the vector formed by (σ_m , σ_a). The vector must be inside the safe area, to obtain a construction that is able to withstand the stresses and which will work for the expected lifetime.

3.2.4 Stresses in 3D

When studying a problem in more than one dimension, the forces can be distributed perpendicular to and/or parallel to a face of the material. The first case will cause normal stresses and the latter shear stresses. (Lund 2005)

It is possible to find an equivalent stress that describes the total impact of the stresses when they appear in 2 or 3 dimensions. It is called “von Mises stress” and the formula can be seen in Eq. 3.34. (Lund 2005)

$$\sigma_e = \sqrt{\sigma_x^2 + \sigma_y^2 + \sigma_z^2 - \sigma_x\sigma_y - \sigma_y\sigma_z - \sigma_z\sigma_x + 3\tau_{xy}^2 + 3\tau_{yz}^2 + 3\tau_{zx}^2} \qquad \textit{Eq. 3.34}$$

where

τ = Shear stress [Pa].

σ = Normal stress [Pa].

x = Subscript describing coordinate in the absorber plane perpendicular to the tubes

y = Subscript describing coordinate in the absorber plane parallel to the tubes

z = Subscript describing coordinate perpendicular to the absorber plane

Moreover, the existence of shear stresses is only a matter of choosing a coordinate system; If a piece of material, in a defined coordinate system A, is exposed to both normal stresses and shear stresses, it is possible to find a new coordinate system B, where the only stresses are (new) normal stresses and all shear stresses are 0. (Lund 2005)

3.2.5 Finite element analysis

For a simple case such as a rod with a single load, the behaviour is predictable using formulas such as Eq. 3.30 to Eq. 3.33. But there will be concentrations of stresses in some parts of the construction when these are more complex, are constructed in different materials, have advanced geometries, and where the load is distributed as a pressure affecting only parts of the construction. Therefore it will be very difficult to predict the mechanical behaviour using manual methods.

By finite element analysis, it is possible to obtain information about the mechanical behaviour in more advanced problems. The technique is to divide the construction into smaller pieces and solve an equation system where the problem is formulated as elements and nodes; the connections between the pieces become nodes and the pieces between the nodes are elements. This is analogous to the heat transfer model, mentioned in “3.1 Thermal model” on page 19. Each part can still be calculated with simple formulas such as Eq. 3.30 to Eq. 3.33. Finite element analysis programs have already been developed to solve problems like this, and the most convenient way of finding the stresses is using such a program. Here, a program called “MSC Marc Mentat” version 2005r2 (32bit) (abbreviated to Marc in this text) is used.

3.2.6 Meshing the geometries

A mesh, as in Figure 3.14 was set up in the finite element analysis program. As can be seen, the mesh only contains the stressed components in the solar collector, namely: cover glass, absorber and tubes.

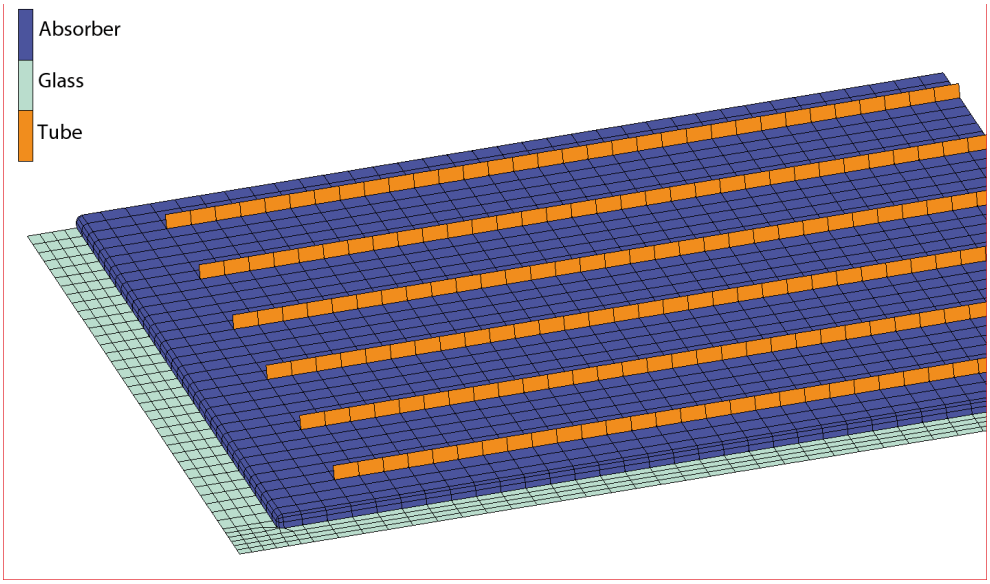

Figure 3.14 *The mesh of the examined part of the solar collector model, upside down*

The elements were meshed as "thick plates" using Mindlin's plate theory (Sunnersjö 1992). As the different parts had different thicknesses they were grouped as "Absorber", "Glass" and "Tube". Because the collector is symmetrical about the x and y axes, only a quarter was actually meshed during the investigation. The model was a simplification of a real solar collector in several ways; the insulation and the outer case were omitted, since they would not be a part of the construction that would have any influences on the stresses due to the gas filling. In the model used it was also assumed that the connections between the different absorber pipes are not part of the absorber. Another simplification was to allow the tubes to be represented by rods; which is possible, if the dimensions of height and width are selected so they will be subjected to the same maximum stress and have the same section modulus. Further information on how the dimensions of the rods were calculated can be read in Vestlund et al. (2011a).

3.2.7 Mechanical properties

As can be seen in Table 3.2, the model in Marc also needed the mechanical properties for the parts.

Table 3.2 Properties of materials in solar collector

Property	Glass	Copper	Aluminium
Young's modulus (GPa)	69	118	70
Poisson's ratio (-)	0.23	0.30	0.30

Poisson's ratio is a way of describing how a material will behave when it is compressed in one direction. Poisson's ratio is defined as the ratio of transverse to longitudinal strains of a loaded specimen. (Lund 2005)

3.2.8 pressure and boundary conditions

In order to cause movement and stresses in the model, a load also has to be applied. The load in this case will be the pressure inside the cavity and the explanation is as follows:

The enclosed gas will act according to the ideal gas law, shown in Eq. 3.35 (Alvarez 1999).

$$p\,V = n\,R\,T \qquad \textit{Eq. 3.35}$$

where

p = pressure(, absolute) [Pa]

V = Volume [m^3]

n = Amount of the gas [moles]

R = Gas constant [8.314472 $J \bullet K^{-1} \bullet mol^{-1}$]

T = Absolute temperature [K]

If the gas is enclosed, the amount of the gas is constant. Then the product of pressure and volume will be proportional to the temperature. When the temperature rises, the gas will expand but, in addition, the box will also offer some mechanical resistance. The resistance will cause the gas to build up a little

pres-sure to enlarge the cavity in the collector box. The pressure will be a variant of the load and Eq. 3.30 to Eq. 3.33 will still be valid. The gas will therefore partly expand and the pressure will increase.

In Marc, it was possible to apply pressure on elements as a boundary condition and then, of course, the boundary condition was only set for the elements that were exposed to the cavity. It was possible to adjust the pressure, by a few iterations, so the product of pressure and volume corresponded to a given temperature.

In addition to the pressure, the double symmetry axes also caused some boundary conditions. Nodes along the x and y axes respectively were set so that they would always keep on the axes and they were not allowed to rotate along the axes, though other movements were allowed.

3.2.9 Calculation and post-processing

It was possible to start the calculation when the mesh was set up, the element types were selected, the mechanical behaviour was given to all elements and the Boundary conditions were set for concerned nodes. The calculations were started with a "Submit" button and, if no errors were detected, there was a result within a few seconds.

During the post-processing some parameters were of interest and therefore studied; they were the volume of the stressed construction, the stress by itself and the movements. First the volume was checked, which, usually gave a new pressure for a new setting of the Boundary condition, but after a few iterations the pres-sure and the volume corresponded well for the required temperature.

The result from the mechanical model was the maximum von Mises stress (mentioned in "3.2.4 Stresses in 3D" on page 34) in each part (glass, absorber and tubes). The von Mises stresses could be visualised in Marc as in Figure 3.15.

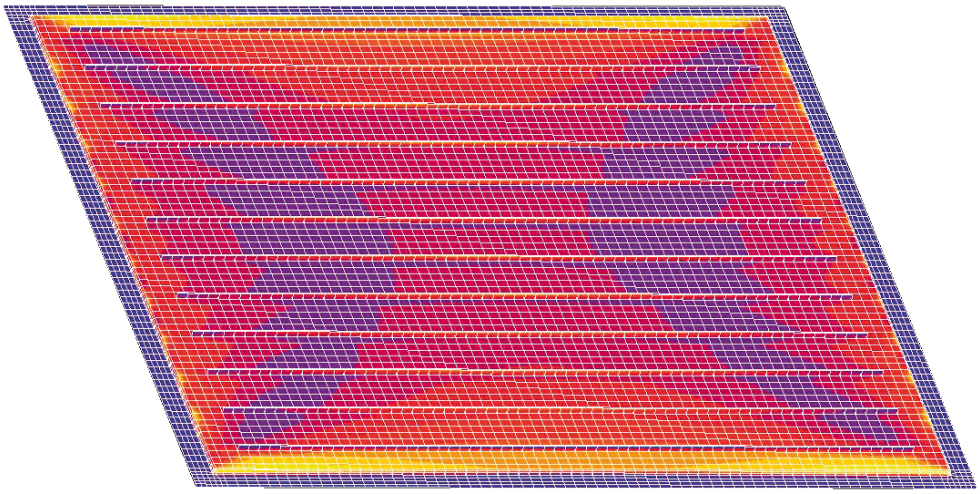

Figure 3.15 *A visualisation of the stresses in colours, where blue shows low stresses going over to red, further to yellow representing the highest stresses*

The figure shows a big, full plate model, only assembled for illustrative use. The actual research is based on a quarter model.

The movements due to expansion/contraction of the enclosed gas were distributed unevenly over the absorber area. Therefore, a description of the distribution was made and sent to the thermal model. The 3d model of movements was made by taking the displacements in the z direction from the mechanical model in Marc. The z direction describes the size of the distance between absorber and glass. An example of the topography of the movements is shown in Figure 3.16.

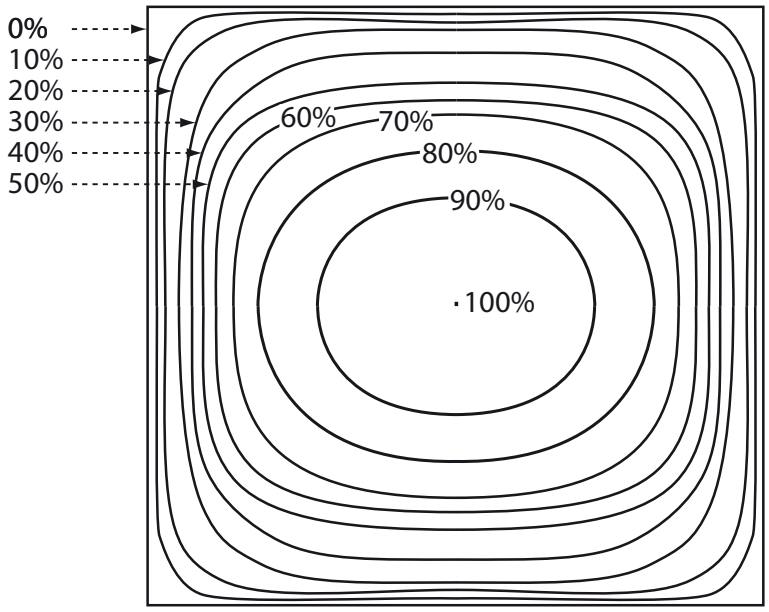

Figure 3.16 *A visualisation with contour lines of the topography of the changed distance between absorber and glass for a solar collector when the temperature inside the collector is changed. Largest distance in the middle*

Marc proposed a 10 contour interval when describing the displacements in the z direction, and the relative area of each interval was passed to the thermal model for more correct calculation of the thermal performance.

3.3 Model validation

3.3.1 Reference collectors

The calculations were compared with empirical data from two commercial solar collectors called Reference 1 and 2 in the following. Reference 1 was an argon-filled, sealed collector (Buderus 2005). Reference 2 was a good quality, normal, i.e. open, air-filled, collector (Quicklund and Johansson 2004)

3.3.2 Thermal model

The deviations in thermal performance between modelled collectors and real performance of the reference collectors were presented in Vestlund et al. (2009) and in Vestlund et al. (2011b). The deviation in thermal performance was smaller in the later article. This can be explained in two ways:

1. The thermal model was, as described in 3.1.6 on page 30, developed during the work of the thesis. Some temperature distributions were assumed in the early versions of the model and actually measured in later versions.

2. The simulation conditions were also revised between the articles mentioned. In Vestlund et al. (2009), data for frequently occurring Swedish weather conditions was used, i.e. irradiance of 800 W/m^2 and an ambient temperature of 0 °C. In Vestlund et al. (2011b), more commonly used test conditions were used where irradiance was 1000 W/m^2 and the ambient temperature was 25 °C.

3.3.3 Mechanical model

The movements due to the temperature in the enclosed gas in reference 1 were compared with those in the model, and the distribution and the sizes of movements showed good agreement (Vestlund et al. 2011a).

A direct validation of stresses was more difficult. This depended on several factors. First of all, it is hard to locate where the maximum stress occurs in a complex construction. Secondly, it is difficult to apply strain gauges. The strain gauges measure elongation but the sources of errors are many, such as bending in the construction and the influence of the heat expansion in the measured material, the strain gauges and in the adhesive of the gauges.

An indirect validation of stresses was, however, possible: The movements of the collector appeared to be similar to those in the model; by the relations presented by Eq. 3.30 to Eq. 3.33 it is possible to find the approximate stresses, depending on the resolution of the model. The model also showed that the reference collector has a reasonable factor of safety, which indicates that the model has been set up correctly.

4. RESULT

The result section gives a brief overview of the more important observations. More details may be found in the articles in the appendixes.

4.1 Thermal performance

4.1.1 An overview of thermal losses

As all thermal transfer is based on temperature differences, a survey is given of the temperatures from the inside to the outside of the solar collector. Figure 4.1 shows the mean temperatures of a normal, air filled, flat plate solar collector, calculated in the simulation model used in this work (Gas-filled, flat plate solar collectors).

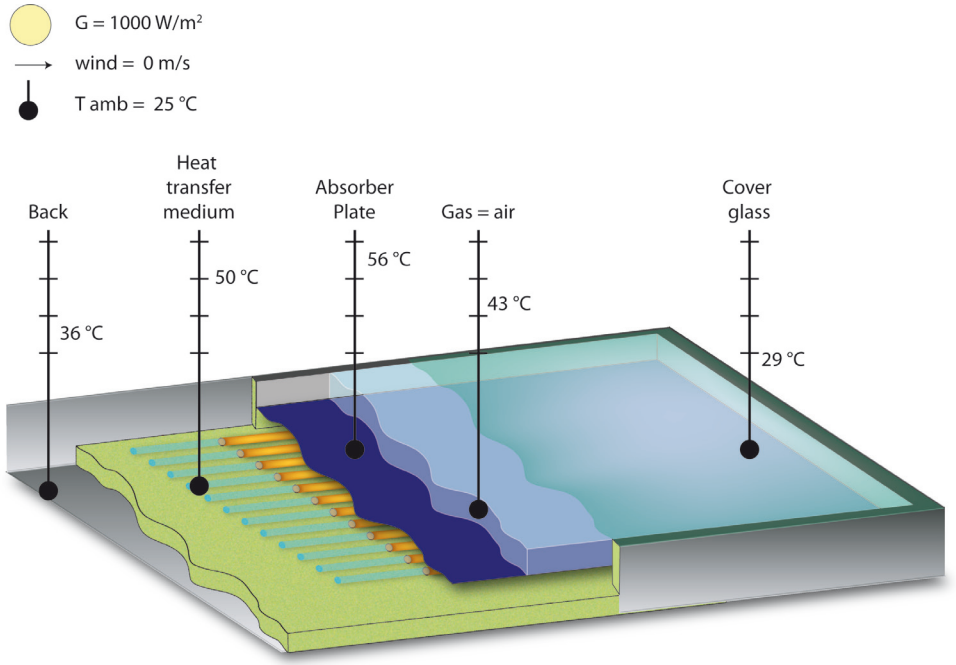

Figure 4.1 Temperatures of different parts on and inside a solar collector

In normal operation, as illustrated in the above figure, the sun shines and the absorber absorbs most of the energy and is heated. The heat will be transferred into the heat transfer medium due to conduction in the absorber and the walls of the tubes.

As can be seen, the absorber has a higher temperature than the heat transfer medium, which is what can be expected; heat transfer relies on temperature differences. However, the figure also shows there are enhanced temperatures in the cover glass and the back, which indicates that there will be some unwanted heat transfer out to the ambience.

More information will be given by a more detailed heat transfer analysis. Table 4.1 shows the actual heat transfers in the collector shown in Figure 4.1.

Table 4.1 Power transfers in a normal, commercially produced air filled flat plate solar collector

Relation	Optical [W/m^2 absorber area]	Conduction/convection [W/m^2 absorber area]	Radiation [W/m^2 absorber area]
Irradiance	1000		
Irradiance falling on absorber	900		
Optical losses	100		
Glass to ambience		13	92
Absorber to glass		94	11
Absorber to tube		771	
Absorber to back		33	
Back to ambience		25	8

The largest heat transfer is the desired transfer from absorber to tube which requires a temperature difference of 7 K.

The optical losses are calculated to be 10 %: 5 % from the glass and 5 % from the absorber. For the upwards losses, the main transfer from the absorber is convectional while radiation is much smaller. The convectional losses can be affected by changing the air to a more suitable gas (see further page 45 in section 4.1.2). Radiation is low due to the low emitting surface of the absorber. From the glass, however, the opposite is true: high radiation losses and low convectional losses. This is explained by high emittance from the glass, and the sky radiation temperature reduction; 10 K reduction relative to ambient temperature was used in the model (Duffie and Beckman 2006). Due to the heat convection

film on the outer surface of the glass, the temperature difference is only a few degrees above ambient temperature.

For the back losses, the first transfer from the absorber to the back plate through the insulation is counted as conduction. The next part is the heat transfer to the ambience. On the back convection dominates, but since the back is at an angle of 45° to the horizontal, i.e. not exposed to the sky, there will not be the same convection as from the front, so the heat convection remains modest although the back has a higher temperature than the front. This also means that there is no sky radiation temperature reduction and radiation is, therefore, also much lower.

Amount of gas

The distance between absorber and glass (d_{pc}) is an important aspect for the gas filling: As Figure 3.4 showed, the noble gases included in the study all have lower conductivity than air. But the other material properties in the same figure which affected convection according to Eq. 3.20 - Eq. 3.23, indicated that the Nusselt number will be higher for the same distance. Therefore it is interesting to analyse the influence of d_{pc} on the thermal performance. Figure 4.2 shows the efficiency of an enclosed solar collector vs the relative gas volume.

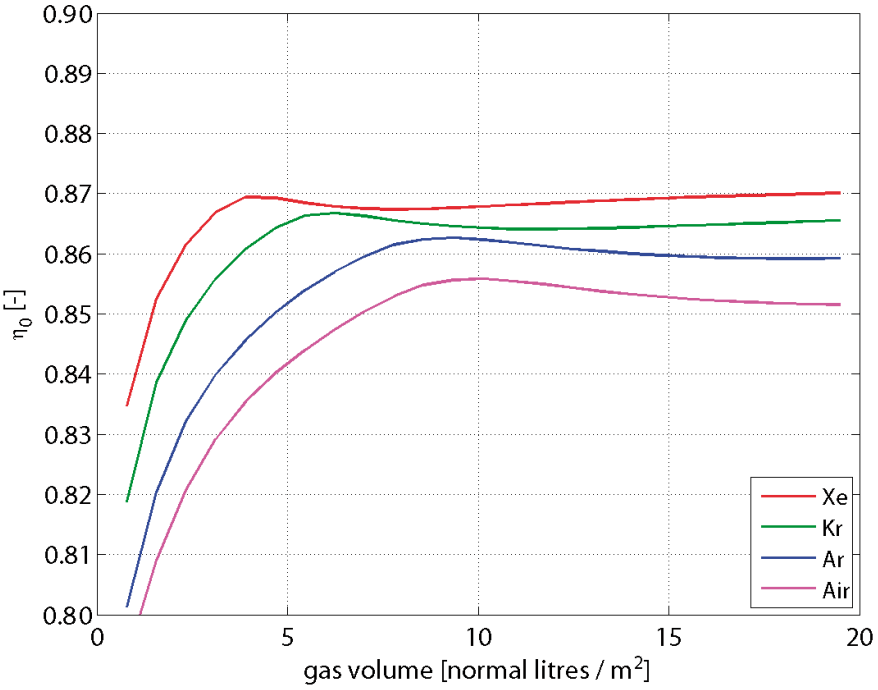

Figure 4.2 Efficiency as a function of the relative gas volume for different gases

The scale of the x-axis in the figure is in normal litres / m^2, where 1 normal litre is the volume of the gas at 25 °C, 100 kPa. For more information on the selection of quantity see Vestlund et al. (2011b). The heat transfer media temperature = ambient temperature = 25 °C.

The figure shows that the different gases retain their positions relative to one another regardless of the gas volume, i.e. xenon is always the most efficient, followed by krypton, argon and air which is the least efficient. It can also be seen, that there is a maximum efficiency for each gas. The volume giving the maximum efficiency, which is determined by the distance between the glass and absorber, is greatest for air and the better the gas with respect to conductivity, the smaller the volume required for maximum efficiency. This could also be foreseen by analysing the material properties and the formulas.

The optimal gas volume and achieved performance is compiled in Table 4.2.

Table 4.2 η_0 with an optimised gas volume

Gas	η_0 [%]	Gas volume [nl/m^2]	Copper use [kg/m^2]
air	85.5	9.3	3.8
argon	86.3	8.6	
krypton	86.6	5.7	
xenon	86.9	3.9	

4.1.2 Temperatures and heat transfer inside a gas-filled, collector

It is important to know how heat is transferred within a solar collector. A model was set up to describe the temperatures and the heat transfers through a cross section of the collector from fin to heat transfer media, where the temperature of the heat transfer media was 50 °C. The model was set up with 10 fin nodes per tube node, and a tube node was selected for observation where the temperature of the tube node was 50 °C (i.e. in the heat transfer medium). The result is visualised as a Sankey diagram in Figure 4.3.

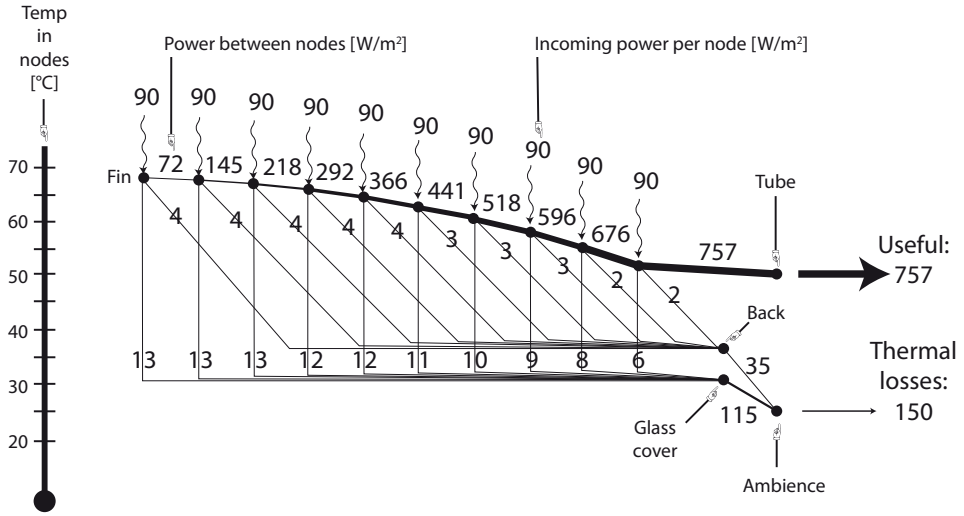

Figure 4.3 A brief description of heat transfer inside a solar collector

The solar collector calculated, is similar to reference 2, which is an air filled, open cavity collector, with a 0.25 mm thick copper absorber, 120 mm centre to centre distance between the parallel sections of the tube which is laid in a meander pattern. The tube is made of copper with an outer diameter of 12 mm and a material thickness of 0.75 mm.

Figure 4.3 is a Sankey diagram where the thickness of the lines represents the power in the elements between the nodes. It also has an extra function where the y-position represents the temperatures in the nodes.

As can be seen in the figure, the incoming power to the ten nodes is 900 W/m^2 totally; the irradiation is 1000 W/m^2, but 100 W/m^2 is lost in optical losses which are not included in the figure.

Some observations:

The temperature difference between the fin nodes increases as the distance to the tube decreases. This indicates that the heat transfer is larger nearer the tube.

The raised temperature furthest out on the fin also influences the back and front losses; the outmost fin node has a loss of 13 + 4 = 17 W per m^2, while the corresponding figure for the node nearest the tube is 2 + 6 = 8 W loss per m^2.

There is a temperature difference of 18 K between the outmost node and the heat transfer media. The temperature difference is explained by the heat transport from the fin to the heat transfer media. If the air in the cavity is changed to a gas with lower heat transfer properties, the thermal losses from the front will decrease; for instance, the xenon filled collector in Table 4.2 on page 47, gives a heat loss of 65 W/m^2 totally, instead of the 115 W/m^2, which was given by reference 2. The fin temperature will thereby increase: The heat resistance in the fin is still the same, and the larger the heat transfer in the fin, the higher the temperature difference between the nodes. The heat transfer media temperature was 50 °C (as mentioned earlier). An unwanted side effect of this also occurs: The heat transfer to the back will increase, since the fin gets warmer; in the xenon case, the temperature rise along the fin will be 20 K, instead of 18 K. Therefore, the back loss goes up from 35 to 36 W/m^2.

The temperature gradient along the fin will become even greater if the thickness of the fin is reduced (compared with the previous case). For instance, if a xenon filled collector with a 0.1 mm copper absorber is substituted for the collector with a 0.25 mm absorber used above, the temperature rise is 41 K, which increases the losses from the front to 92 W/m^2 and from the back to 50 W/m^2, (142 W/m^2 in total). But this is still better than the air filled collector shown in Figure 4.3, which had a total loss of 150 W/m^2.

4.1.3 General optimization of the use of copper

An optimization showed how the total use of copper in a solar collector can be used in a more efficient way. The thickness of the absorber is traditionally 0.25 mm when copper is used (Konttinen 2007). If the absorber thickness (d_p) and the tube to tube distance vary (d_{tt}), the result will be as shown in Figure 4.4.

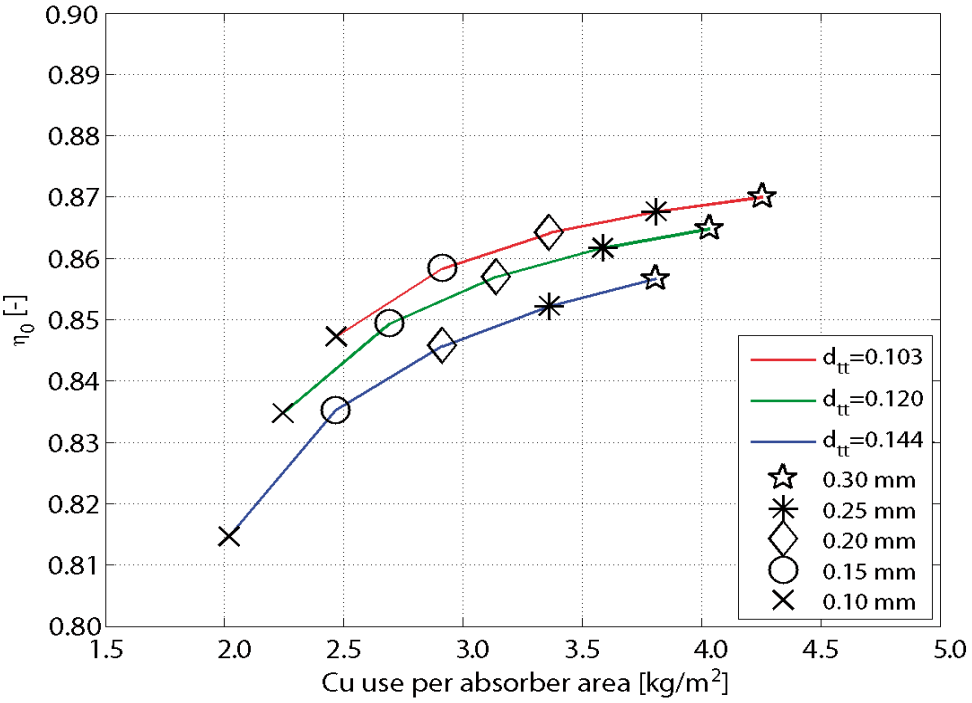

Figure 4.4 *Influence of use of copper (absorber thickness and tube spacing together) on efficiency for an argon filled collector*

The figure shows the result of calculations with 12 mm copper tubes with a material thickness of 0.5 mm and argon gas. For other gases, the actual performance will differ but the curves will be similar.

As can be seen, the best performance per amount of copper used is reached by using the shortest studied distance between the tubes together with a thinner absorber. It would, for example, be possible to reduce the use of copper for the argon filled collector in Table 3.2 from 3.8 kg/m^2 down to about 3.2 kg/m^2 and still achieve the same performance by reducing absorber thickness to 0.18 mm from 0.25 mm and the centre to centre distance of the tubes to 103 mm from 120 mm.

The optimization of the use of copper by using thinner absorbers and shorter tube to tube distances also agrees with the results found by Eisenmann et. al (2004).

4.1.4 Overall performance

Gas-filled solar collectors have a potential for saving material and/or achieving better performance. To test the gas-filled collectors and see how they pass the test, an overall performance study was done for the collectors with 0.1 mm thick absorbers (also called lean collectors) and a centre to centre tube distance of 103 mm. Figure 4.5 shows the efficiency curves of those lean collectors and compares them with the two reference collectors mentioned in 3.3.1 on page 40.

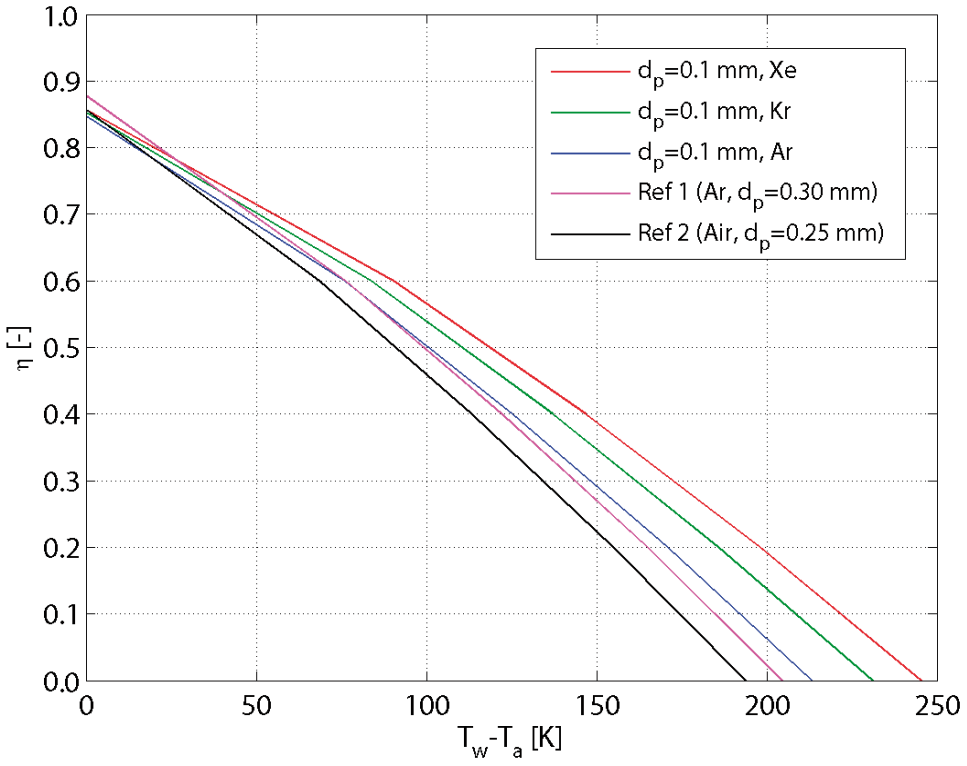

Figure 4.5 *Efficiency curves for gas filled solar collectors with a copper absorber thickness of 0.1mm, compared with two reference collectors*

The collectors with 0.1 mm absorbers (lean collectors) start at T_w-T_a = 0 with a modest η_0 , similar to the references. At higher temperatures however, the lean collectors all have higher efficiency than the references and the stagnation temperatures are considerably higher in all the noble gas filled collectors. This

is also true for the argon filled, lean collector in comparison with reference 1 although they are both argon filled; the main reason is simply that the lean collector uses a more optimal amount of gas, as described in 4.1.2.

The data on the lean collectors are compiled in Table 4.3.

Table 4.3 Performance of the lean collectors v.s. the references

Denomination	Ar,Cu0.1	Kr,Cu0.1	Xe,Cu0.1	Reference 1	Reference 2
Gas	argon	krypton	xenon	argon	Air (open)
η_0 [%]	84.7	85.2	85.6	87.4	85.6
$\eta((T_w-T_a)/G=0.25)$ [%]	77.7	78.4	79.6	79.3	77.3
$\eta((T_w-T_a)/G=0.50)$ [%]	69.5	71.4	72.7	70.1	67.6
a [W/m^2K]	3.01	2.76	2.56	3.40	3.54
b [W/m^2K^2]	0.00458	0.00407	0.00380	0.00429	0.00460
Copper usage [kg/m^2]	2.5	2.5	2.5	5.0	4.2

When comparing Table 4.2 on page 47 with Table 4.3, it can be seen that the lean collectors will have a slightly lower η_0. For example, the η_0 for the argon filled collector will be 84.7 % instead of 86.3 % (Table 4.2 on page 47). because the fin is less efficient. The reduction in performance for a collector with a thin, 0.1 mm absorber instead of a normal (0.25 mm) thick absorber and with all other properties exactly the same, will be around 2 % in the first, low temperature part of the performance curve for all gases examined, ($0 \leq (T_w-T_a)/G \leq 0.50$). However the difference will decrease at higher temperatures, since the heat transfer in the fin decreases. At stagnation temperature there is no heat transfer at all in the fin, which means that the stagnation temperature will be the same regardless of the thickness of the absorber.

When comparing the different solar collector configurations in Table 4.3, it is clear that the gas filling in the collectors has become more important for $\eta((T_w-T_a)/G=0.50)$ than it is for η_0. The influence of the thin fin reduces the performance by around 2 %, but, as shown in the table, the air filled reference

2 has decreased its efficiency to 67.6 % while the lean, gas-filled are 2 to 4 % better. This shows that the heat transfer properties for the gas inside the cavity have a big impact on the performance, which can also be seen from the a and b values. The performance of all the lean collectors is better than that of the references, except the argon filled lean collector in comparison with the also argon filled reference 1. But the difference between them is only 0.6 % (at η_0 it is 2.7 %).

The use of copper is also an interesting factor: Reference 1 and 2 use 5.0 and 4.2 kg copper per m^2 respectively. By using the lean, gas-filled collectors it is possible to reduce the amount of copper from 5.0 kg/m^2 to 2.5 kg/m^2, a reduction of 50%, while the performance is the same to within a few percent depending on selected gas and temperature

4.1.5 Thermal performance with aluminium absorbers

A further reduction of copper is possible if the absorber is changed to aluminium. Given that copper is still used in the tubes, an alternative is to increase the centre to centre distance of the tubes, preferably together with the thinnest possible material thickness in the tubes. In Figure 4.6 the relation between η_0 and absorber is visualized for different tube configurations and the gas is argon.

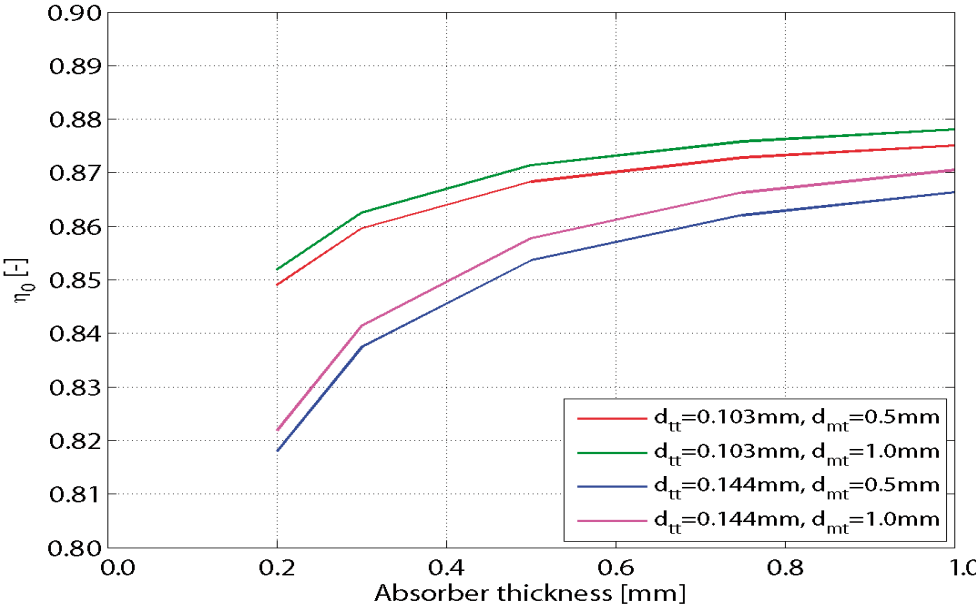

Figure 4.6 *Performance and variations of aluminium absorbers for different tube thickness and centre to centre distances of tubes for an argon filled collector*

In the copper result sections presented earlier, it could be seen that the collector with an argon gas filling and a normal thick copper absorber (Ar,Cu0.25) had an η_0 of 86.3 % and the also argon filled, collector with a thin absorber (Ar,Cu0.10) achieved 84.7 %. If the aluminium absorber collector result is compared with the copper collectors mentioned, it is possible to achieve both those η_0 values or even higher regardless of the centre to centre distance and tube thickness; it is only a question of absorber thickness.

Here, it is also possible to see an improved performance when using 1.0 mm thick tubes instead of 0.5 mm. This depends on the changed Reynolds number inside the tubes when the inner diameter is changed.

With maximum copper reduction in focus, it is of interest to consider the configuration in the figure which uses the least copper. This is represented by the blue curve, which had the longest tube to tube distance (144 mm) together with the thinnest tubes (0.5 mm). The performance reference configurations for argon filled collectors mentioned in sections 3.1.2 and 3.1.5 are compiled and compared in Table 4.4.

Table 4.4 Performance of an aluminium absorber collector with smallest use of copper in tubes studied and comparison with use of copper in collectors with copper absorbers and the same performance

Aluminium use [kg/m^2]	Absorber thickness [mm]	Gas	η_0 [%]	Copper use corresponding copper absorber [kg/m^2]	Corresponding copper absorber collector
2.17	0.80	argon	86.3	3.80	Ar,Cu0.25
1.22	0.45	argon	84.7	2.50	Ar,Cu0.10

The use of aluminium and copper will also be the same when the copper absorbers are replaced in the krypton and the xenon filled collectors. Table 4.4, therefore only shows the result for argon.

As can be seen it is possible to reduce the use of copper significantly; it decreases from 3.8 kg/m^2 (Ar,Cu0.25), (table 4.2) and 2.5 kg/m^2 (Ar,Cu0.25), (Table 4.3) respectively to 1.12 kg/m^2 by using aluminium in the absorber with the same performance as corresponding copper absorber.

Note that the thickness of the tubes and absorber will affect the mechanical behaviour and this will be further analysed in next section.

4.2 Mechanical performance

4.2.1 Stress dependencies of solar collector dimensions

A study was also done in order to find interesting relations between factors of safety and height, width, thickness and selection of material. (Vestlund et al. 2011a) For length and width, the best way was to describe them as absorber area and the angle built by arctan (length/width) as in Figure 4.7.

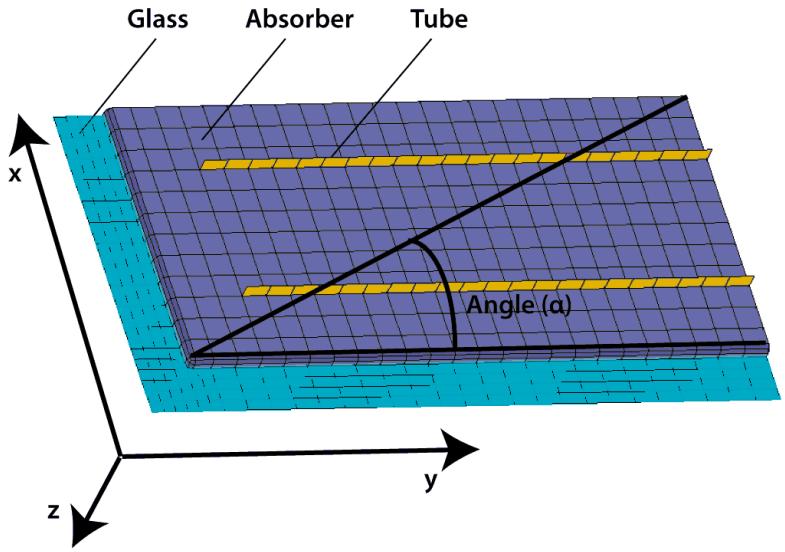

Figure 4.7 *The angle describing the length and width relation*

It is difficult to give any relevant absolute figures in the relation between the smallest factor of safety and the absorber area and angle as it is also dependant on other aspects of the configuration, such as material, thicknesses of the materials, and different geometries. An example of a visualisation of the relation can be seen in Figure 4.8.

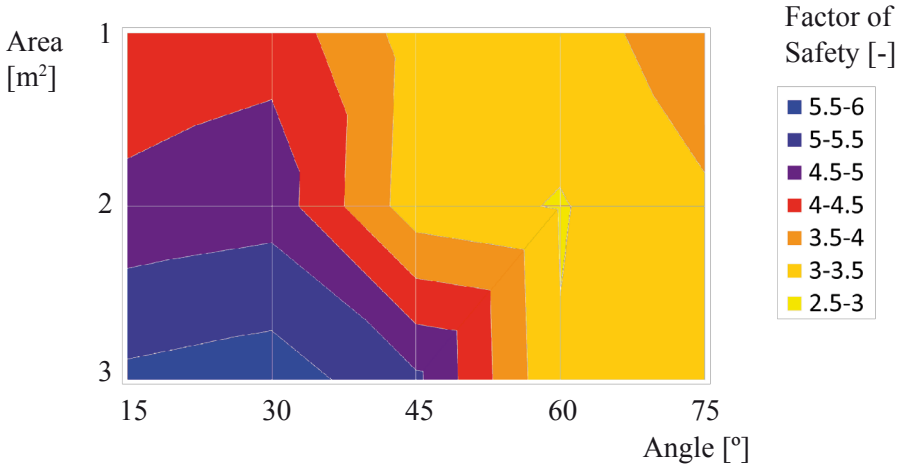

Figure 4.8 *Example of the lowest factor of safety in relation to the collector absorber area and angle defined inFigure 4.77*

The figure is calculated for collectors with the following configuration:

- 4 mm soda-lime glass
- 0.25 mm copper absorber
- 12 mm copper tubes with 0.85 mm thickness and 120 mm tube to tube c/c.
- 10 mm distance between absorber and glass

Although there were many factors to be considered, there were also some general trends (Vestlund et al. 2011a):

1. The shorter the distance between glass and absorber, the higher the factor of safety (FoS). The stress was nearly proportional to the distance. Consequently, the factor of safety is nearly inversely proportional to the distance.

2. The larger the area, the higher the FoS.

3. The smaller the angle (i.e. longer tubes) the higher the FoS.

Another important aspect to consider is that the levels of stresses are unpredictable without a comprehensive calculation. When reinforcing one part of the construction that part will be stiffer, but the gas expansion, when the collector warms up, is nearly the same, so the pressure rises and the stresses increase, i.e. a reinforced construction can have higher stresses.

4.2.2 Stress vs. material and thicknesses of material

When analysing collectors with copper absorbers it was found that it is preferable for the FoS (factor of safety) to use a thinner absorber and a short distance between the tubes, as discussed in the previous section. This can be seen in Figure 4.9, where the calculation is based on an argon filled collector.

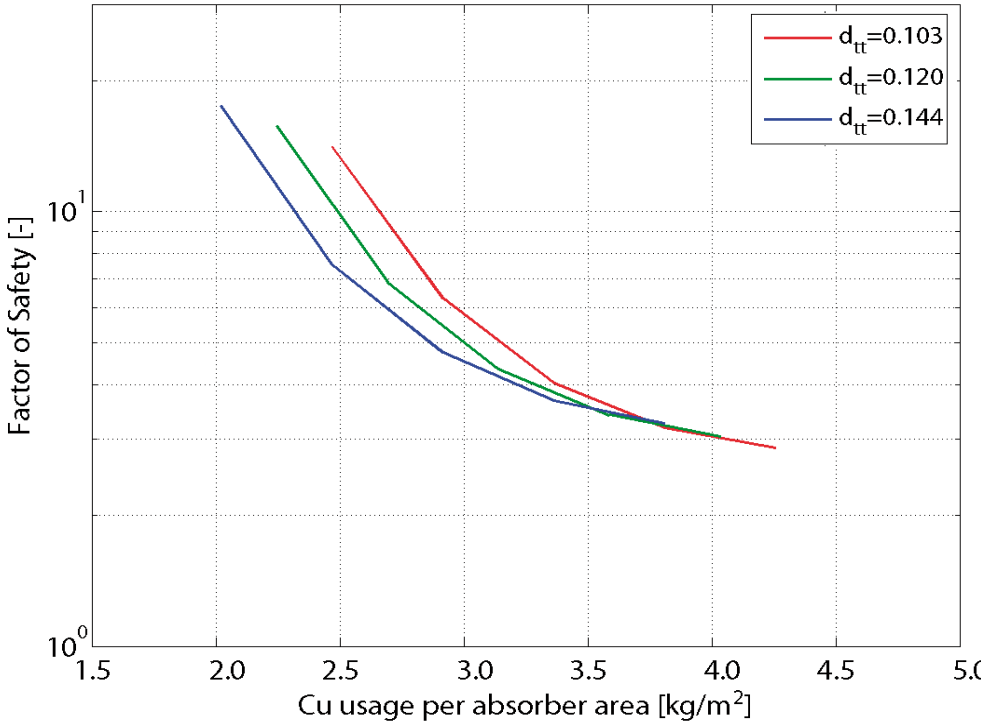

Figure 4.9 *Factor of safety for collectors with copper tubes and absorbers rises the thinner the absorber and the shorter the distance between the tubes*

For the solar collectors which use more than 3.5 kg/m^2 copper, the centre to centre distance between the tubes does not seem to have any significant influence. For solar collectors with a low use of copper (i.e. thin absorber), however, the best factor of safety is achieved with the shortest studied centre to centre distance. This use of a short distance between the tubes together with a thinner absorber to give a better factor of safety coincides with the optimization of performance with respect to reducing the use of copper, see 4.1.3 on page 49.

4.2.3 Mechanical stresses when absorbers in aluminium

The reduction of copper presented in "4.1.5 Thermal performance with aluminium absorbers" on page 52, showed it was possible to achieve the same performance with collectors using aluminium absorbers. The configuration using the least copper of those examined, has a 144 mm tube to tube distance together with 0.5 mm copper tubes.

Figure 4.10 gives a survey of the factor of safety in relation to aluminium absorber thicknesses and different tube configurations.

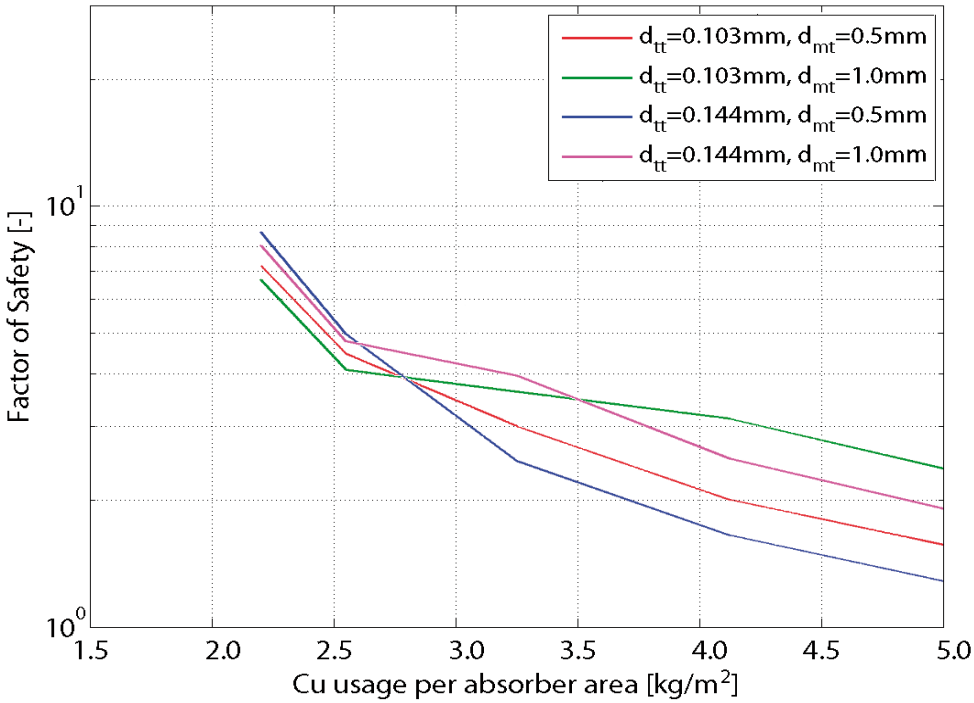

Figure 4.10 *Factor of safety for collectors with aluminium absorbers and copper tubes also rises the thinner the absorber and the shorter the ideal distance between absorber and glass*

The figure shows that the collector with 0.8 mm absorber, mentioned in Table 4.4, will have a factor of safety of between 1 and 2. This may be critical and needs a more detailed analysis, (i.e. better resolution in the model) before it can be used. The 0.45 mm in the same table is however not in any critical zone regarding the factor of safety since it has a value of about 3.

One way of improving the factor of safety can be by using thicker tubes. Figure 4.10 indicates that thicker tubes give a higher factor of safety for collectors with thick absorbers, i.e. those over about 0.4 mm. With the thicker tubes, the collector with the 0.8 mm absorber discussed earlier will have a factor of safety of about 2.5. But the amount of copper used will also increase from 1.12 to 2.15 kg/m^2 and although 2.15 kg/m^2 is less than the 3.8 kg/m^2 that a normal thick copper absorber (=0.25 mm) presented in Table 4.2 uses, it is still not a

very big optimization. Therefore, the collectors with 0.5 mm thick copper tubes are still of interest in order to see if it is possible to improve the factor of safety.

If the gas is changed to krypton instead all factors of safety can be multiplied by 1.5, due to the shorter ideal distance between absorber and glass (see 4.1.2 on page 47 and forward). Then, the FoS will be 1.5 *1.5 = 2.25 and the 0.8 mm absorber can be acceptable. And if the gas is changed to xenon, the factors of safety for argon collectors can be multiplied by 2.2, which improves safety even more (2.2 * 1.5 = 3.3).

4.3 Yield and material cost

To be interesting for commercial production, the gas-filled solar collectors need to deliver acceptable performance, from an economical, as well as an environmental perspective.

In the following, all the collectors (except the references) are configured in the following way: copper absorber collectors use a centre to centre tube distance of 103 mm and the aluminium collectors 144 mm. The tubes have an outer diameter of 12 mm and a material thickness of 0.5 mm. Optimal gas volumes presented in Table 4.2 are used.

4.3.1 Yield estimation

An estimate of the annual yield was made in the same way as calculated in the Swedish subsidy programme. This makes it possible to compare the gas-filled collectors with collectors from at least one market, in this case the Swedish market. The calculation is based on a program from Qaist (2010). It is possible to calculate either with steady state figures according to EN 12975-2, Chapter 6.1, or Quasi Dynamic testing according to EN 12975-2, Chapter 6.3. Here, the steady state evaluation method was used. All calculations use a simple, one direction incident angle modifier with a b0 value of 0.1. The result is presented in Table 4.5.

Table 4.5 Annual yield of gas-filled solar collectors with different configurations

Denomination	Gas filling	Absorber material	Thickness absorber [mm]	Annual yield(1) [kWh/m² aperture]
Xe,Cu0.25	Xe	Cu	0.25	649
Xe,Al0.75	Xe	Al	0.75	643
Xe,Cu0.10	Xe	Cu	0.10	630
Kr,Cu0.25	Kr	Cu	0.25	628
Kr,Al0.75	Kr	Al	0.75	622
Xe,Al0.30	Xe	Al	0.30	620
Kr,Cu0.10	Kr	Cu	0.10	608
Ar,Cu0.25	Ar	Cu	0.25	600
Kr,Al0.30	Kr	Al	0.30	598
Ar,Al0.75	Ar	Al	0.75	594
Ar,Cu0.10	Ar	Cu	0.10	580
Reference 1	Ar	Cu	0.25	575
Ar,Al0.30	Ar	Al	0.30	569
Air,Cu0.25	Air	Cu	0.25	557
Air,Al0.75	Air	Al	0.75	549
Reference 2	Air	Cu	0.25	546
Air,Cu0.10	Air	Cu	0.10	534
Air,Al0.30	Air	Al	0.30	522
Mean value in Swedish subsidy list of flat plate solar collectors				423

(1): Weather data from Stockholm, 50 °C mean heat transfer medium temperature.

The table is sorted with annual yield in descending order, and consists of normal and thick absorbers, copper or aluminium absorber material and 3 different noble gases and for comparison also air filled collectors. This gives 16 test objects. Also for comparison reason the references are calculated and the mean values given from the list of collectors granted a subsidy in Sweden (SP Technical Research Institute of Sweden 2010).

It can be seen that xenon filled collectors come high up on the list; the three first positions are filled by xenon collectors and it is only the collector with

the thin aluminium absorber Xe,Al0.30 that has a poorer yield than the best krypton filled collectors. The krypton filled collectors are in the middle of the range; with a thick absorber they are even better than the Xe,Al0.30, but the thin aluminium absorber Kr,Al0.30 yields more than the best argon filled collector, Ar,Cu0.25. The argon collectors come after that and they all yield more than the air filled collectors. Both the argon filled collector with a thick absorber and the argon filled collector with a thin copper absorber have a better yield than Reference 1 which is also an argon filled collector. Among the air filled collectors, the collectors with thick absorbers are better than Reference 2 which, in its turn, is better than the collectors with thin absorbers. It can also be seen that all the collectors calculated will yield better than the mean value of the flat plate solar collectors.

4.3.2 Production price estimation

Making a price calculation for a potential product is hazardous; the price of the materials inside the collector varies a lot depending on rationality and capacity in production, ability of price negotiations and price fluctuations, delimitations of process and material etc. But as an indicator of what is of interest for further consideration for a potential manufacturer, an approximate estimate will suffice. The figures used are presented in Table 4.6.

Table 4.6 material prices used for a rough cost estimation

Part	Price	Source
Copper	6900 USD / ton	Skandinaviska Enskilda Banken AB (2009)
Aluminium	2300 USD / ton	Skandinaviska Enskilda Banken AB (2009)
Argon	0.024 USD / normal litre	Edlund (2010)
Krypton	0.5 USD / normal litre	Pettersson (2005)
Xenon	1.5 USD / normal litre	Pettersson (2005)
Insulation	83 USD / m^3	Solentek AB (2010)
Glass	24 USD / m^2	Solentek AB (2010)
Back plate	4 USD / m^2	Solentek AB (2010)
Sealing (only the sealed)	3 USD / m	Olofsson (2010)
Selective surface on absorber	10 USD / m^2	Solentek AB (2010)

As the Commodity Market prices quoted are in US dollars, this currency has been used throughout the thesis

With yield figures from Table 4.5, and the prices of the components mentioned above, the total material price in relation to annual yield can be seen in Figure 4.11.

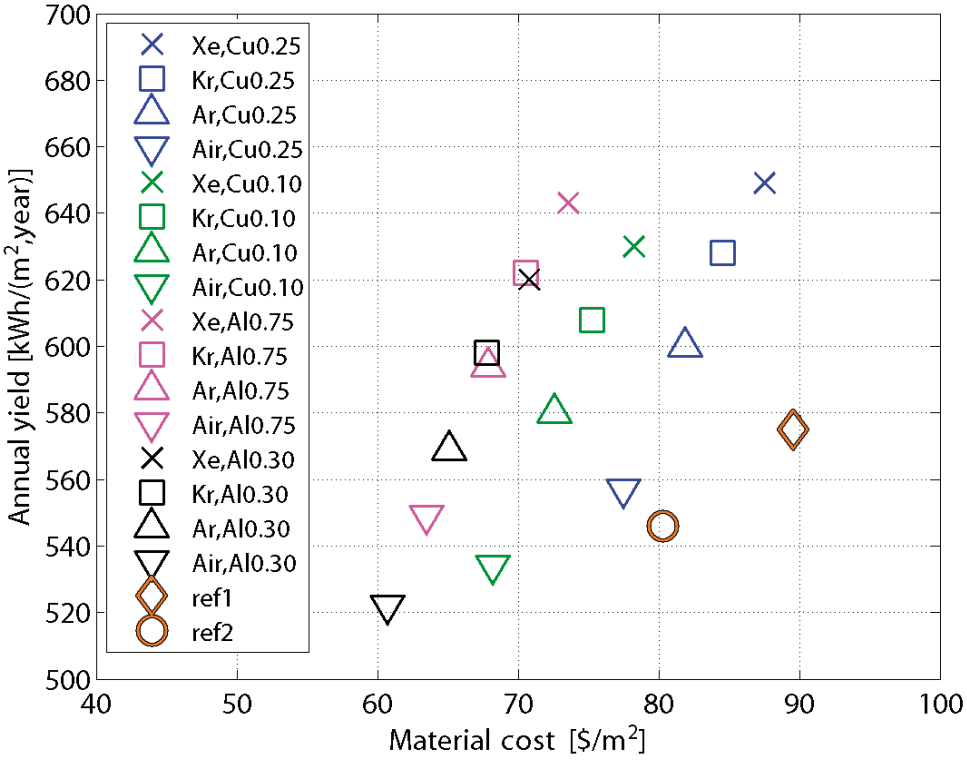

Figure 4.11 Annual yield in relation to material cost in different configurations

The axes are both truncated to make it easier to see the differences in yield and price. The yield differs up to 20% (Xe,Cu0.25/Air,Al0.30) and the material price differs up to 47% (ref1/Air,Al0.30).

The figure indicates that all the collectors with aluminium absorbers give the most energy per material cost, and the annual yield and the material cost form a linear relationship. The collectors with thin copper absorbers form another linear relationship with less energy per material cost and the normal thick form a third, linear relationship with even slightly less energy per material cost. The worst cases are the references.

If the collectors are estimated to be used for 20 years, the yield per assembly cost will be as shown in Table 4.7.

Table 4.7 Energy during 20 year use per material cost

Denomination	Energy per material cost (Annual yield in Stockholm at 50 °C) [MJ/$]	In relation to the best [%]
Kr,AL0.30	635	0
Kr,Al0.75	635	-0.1
Xe,AL0.30	631	-0.7
Ar,Al0.75	630	-0.9
Xe,Al0.75	629	-0.9
Ar,Al0.30	629	-1.0
Kr,Cu0.10	582	-8.4
Xe,Cu0.10	580	-8.7
Ar,Cu0.10	575	-8.9
Kr,Cu0.25	534	-16
Xe,Cu0.25	534	-16
Ar,Cu0.25	527	-17
Ref2	490	-23
Ref1	462	-27

The table confirms what Figure 4.11 indicated; all the collectors with aluminium absorbers give more energy per material cost than those with copper absorbers. For the collectors with aluminium absorbers, the energy per assembly cost is almost the same regardless of the thickness of the absorber and the gas selected. For the collectors with copper absorbers, the use of copper is important and thin absorbers have a better result. The thin copper absorbers give 9 % less than the aluminium, and the normal thick copper absorbers give about 16 % less. Selection of gas has very little influence on the result. It can also be seen that all the tested collectors give more than either of the references.

An analysis was also made to estimate the material cost sensitivity, which can be seen in Table 4.8.

Table 4.8 Impact of total material price if the price of a part is changed

	Cu in abs and tubes	Al in abs	Gas	insu-lation	glass	box	seal-ing	sel surf
Ref2	0.36	0.00	0.00	0.04	0.30	0.17	0.00	0.12
Ref1	0.38	0.00	0.01	0.04	0.27	0.15	0.05	0.11
Ar,Cu0.25	0.32	0.00	0.00	0.04	0.29	0.17	0.05	0.12
Kr,Cu0.25	0.31	0.00	0.03	0.04	0.28	0.16	0.05	0.12
Xe,Cu0.25	0.30	0.00	0.07	0.04	0.27	0.16	0.05	0.11
Ar,Cu0.1	0.24	0.00	0.00	0.05	0.33	0.19	0.06	0.14
Kr,Cu0.1	0.23	0.00	0.04	0.04	0.32	0.18	0.06	0.13
Xe,Cu0.1	0.22	0.00	0.07	0.04	0.31	0.18	0.05	0.13
Ar,Al0.75	0.11	0.07	0.00	0.05	0.35	0.20	0.06	0.15
Kr,Al0.75	0.11	0.07	0.04	0.05	0.34	0.20	0.06	0.14
Xe,Al0.75	0.11	0.06	0.08	0.05	0.33	0.19	0.06	0.14
Ar,Al0.3	0.12	0.03	0.00	0.05	0.37	0.21	0.06	0.15
Kr,Al0.3	0.11	0.03	0.04	0.05	0.35	0.20	0.06	0.15
Xe,Al0.3	0.11	0.03	0.08	0.05	0.34	0.19	0.06	0.14

Each material's share of the price is presented in the table, and this also means that it is possible to see the sensitivity. If, for example, the price of copper rises by 20%, then the material in "Kr,Al0.3" will be 0.11*20%=2.2% more expensive, while "Ar,Cu0.25" will be 0.32*20%=6.4% more expensive.

4.3.3 Energy demand of production

One aspect of solar collector performance is the environmental load. A study was carried out in order to give a rough estimate of the primary energy demand for manufacturing the collectors.

The question of energy demand of production is complicated. Solar collectors are not a complete energy system in themselves, but are part of a larger energy system. This means that the energy demand for the production of a complete energy system is larger than that of the collectors alone. On the other hand, the solar heating system can replace other heating equipment and the energy saved

by not producing that equipment can be saved. This comparison only describes the energy demand of different designs of flat-plate solar collectors, and the figures used are presented in Table 4.9.

Table 4.9: Energy demand for different materials in a collector

Part	Energy demand	Source
Copper (DE-mix-2010)	48000 MJ/kg	Öko-Institut (2010)
Aluminium (import-mix-DE-2010)	183000 MJ/kg	Öko-Institut (2010)
Argon	0.672 kJ / normal litre	Weir and Muner (1998)
Krypton	38500 kJ / normal litre	Weir and Muner (1998)
Xenon	511400 kJ / normal litre	Weir and Muner (1998)
Insulation	14 MJ/kg	Öko-Institut (2010)
Glass	11.9 MJ/kg	Öko-Institut (2010)
Back and edge (1.5 mm aluminium, import-mix-DE-2010))	183000 MJ/kg	Öko-Institut (2010)

Figure 4.12 shows the yield figures from Table 4.5, in relation to the energy demand of the components mentioned above.

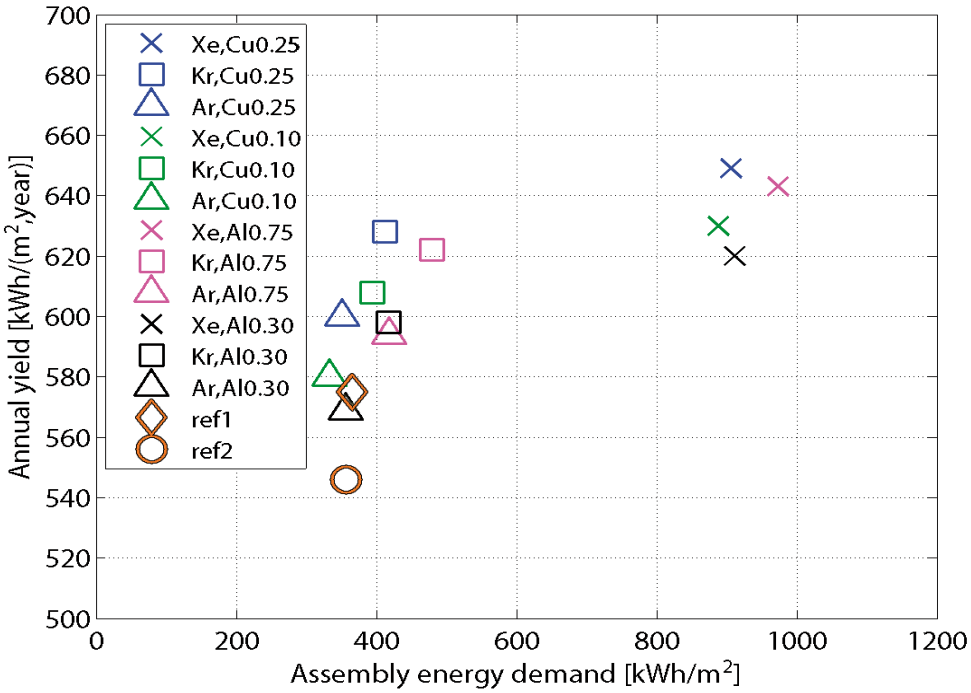

Figure 4.12 *Annual yield in relation to energy demand for manufacturing a collector*

It is notable that all the xenon filled collectors have a higher energy demand than the other collectors. Krypton, however, has more impact on the performance than on the energy demand, while an aluminium collector with about the same annual performance as a copper collector has a larger impact on the energy demand.

It shall be remembered that even though the units are the same on both the axes of the diagram, they are still not comparable. The assembly energy demand is primary energy, but the energy the solar collector replaces is not, which means that the replaced primary energy will be different. The benefit will, for example, be greater if the energy replaced would have come from an electric heater and this electricity had been produced with a low efficiency factor.

5. DISCUSSION

5.1 Validation and precision in models

The validation showed good agreement between models and references. However, several points must be considered regarding validation.

There are several possible sources of error: 1), lack of precision in the formulas describing the physics, 2), lack of precision in measurements of the references, 3) lack of adequate information about the references, 4), truncation errors in the model. However, as the models only consist of formulas and no calibrations are carried out there cannot be any calibration errors.

It is noteworthy that validation is a comparison between two results, both of which are based on measurements: The data and formulas that describe the physics originate from measurements that are extracted from experiments based on many measurements in research carried out by other researchers. Solar collector tests are also based on measurements.

It is important to remember that as long as the validation gives a few percent difference, it is hard to explain the reason for the difference. It is not even possible to trust a near zero difference since the deviations can neutralize each other as well as concur.

In general it may be said that if the difference in the validation is large, it is probable that either there are bugs in the model, or that some assumptions are wrong (absorbtance and emittance are, for instance, both assumed), or the model is too simple. When developing the thermal model, differences most often depended on a program bug, and in the mechanical model strange results depended on wrong properties being set for some part of the collector.

5.1.1 Data sources

When analysing the reliability of sources, it is interesting to study the motivation of the person publishing the result. There may have been pecuniary interests or a wish for recognition behind the publication. This study is based on well established table data and formulas describing the physics, and there are no reasons for suspecting any big deviations arising from these. Knowledge of thermodynamics, for example, was originally needed to develop better steam engines, but it is hard to find any commercial or other interest for enhancing

any data on the physical behaviour of the materials used. Therefore, there is no reason to pay extra attention to the academic colleagues who have carried out this impressive work.

Another relevant consideration is which formulas should be used. The thermal calculations in this study are based on formulas described by, for example, Duffie and Beckman (2006) and Holman (2002). The formulas calculate heat transfer by using physical dimensions, gas properties and temperatures as input, and were setup as a calculation system described in 3.1.3 on page 25 and onward. The formulas used are, however, not computational fluid dynamics (CFD), where the calculations are based on the actual movements within the fluid. As the selected method gave an accuracy of within a few percent, it was judged to be sufficient for the purpose of calculating the thermal behaviour of gas-filled collectors, but if the resolution needs to be higher, CFD would be an alternative.

The models have been validated with measured figures taken from energy declarations by Quicklund and Johansson (2004) working at the Technical Research Institute of Sweden (SP) and Institut für Solarenegieforshung GmbH (2001).

5.1.2 Lack of data

Some data regarding the references were missing or only given in an interval with an under and an upper limit. Commonly occurring values were substituted for missing data on properties, and a median value for missing data for intervals. It is, however, important to note that these values remained unchanged during the experiment when changing gas unless otherwise described.

5.1.3 Models

The models can calculate reasonably accurately which means that the truncation error is small enough for the purpose compared with the input data errors mentioned above. There are several reasons for not trying to reduce the truncation error more than to a certain level: firstly, an overambitious reduction of the truncation error would be futile since the errors in input data would still remain even if the truncation error were small. Secondly, the calculation time increases by the square of the number of nodes (if the number of nodes is n, then the size of the relation matrix described in Eq. 3.26 will be n x n). The third reason for making simplifications is the time aspect; more complicated models can give improved precision but there are difficulties in setting up these

models; solving the difficulties takes a lot more time and the improvement is limited.

When making simplifications, only those with no or limited impact should be implemented. An example of a trifling simplification is in the thermal model where the absorber is counted as if the fin were not connected to the neighbour fin as it would actually be in a full plate solar collector. This is, however, the case for all models tested here, including the references, and is not gas specific, so it is estimated that this simplification does not affect the result or the internal order very much, if at all. Another example of simplification was when the bends in the tubes were omitted in the mechanical model. They do have less influence, as mentioned in "1.2.5 Limitations" on page 7, but it is difficult to give the exact figure, unless a model is set up, and there were other priorities for the use of time in this project. These simplifications mean that the results of tests on the model are not completely accurate, but the worst pitfalls can be avoided; this is, moreover, the reason for using a greater factor of safety than 1. A refinement of the mechanical model would perhaps give more detailed information about the stresses, but this project must also be limited at some point and this is a question of priorities, as mentioned in 3.3.3.

It is interesting to consider the number of nodes. The thermal model worked well when the number of absorber nodes per tube node was 4, and the number of tube nodes was 3 (i.e. two nodes where heat was delivered to the heat transfer media and one for the incoming heat transfer media). If the number of nodes increased over these figures, the result hardly changed at all. This indicates that the nonlinear behaviour along a cross section of the fin is more important than the nonlinearities due to the heat added along the tube.

For the mechanical model, there are problems of transparency depending partly on the use of a commercial finite element analysis program where calculation in the program cannot be followed, and partly on the indirect validation described in "3.3.3 Mechanical model" on page 41where the problem is to make direct measurements of stresses. Finite element analysis is, however, a well established technique and there is little reason to suspect that a program would fail to solve a problem that would be described as simple compared to the full potential of the program.

5.2 Assessments of the energy demand

Life cycle assessments (LCA) can provide quantification of environmental impact; the impact that raw material extraction, energy production, manufacturing processes, transportation needs and waste disposal requirements have on both social and natural environments (Weir and Muneer 1998). However, all figures contain uncertainties, such as the deviation due to local variations of the supply of energy for extracting and refinements (Baumann and Cowell 1999). The study concentrated on considering the energy demand of manufacturing the solar collectors described. The metals used are a mixture of virgin and recycled materials, where the proportions correspond to the availability in Germany. The rest of the materials used are virgin materials. The gases are, for example, extracted directly from air. This implies that LCA studies are only rough estimates, and if other sources or other Boundary conditions were to be set, other figures would also be presented.

The study did not look at the energy demand at the end of the life cycle, because this part is even more uncertain. For land filling only, the energy demand is small, and for recycling, most of the energy for manufacturing new products will be counted as an energy demand for the new products. Baumann and Tillman (2004) also pointed out that a limited study that focuses on the essentials can give a clearer result.

The study shows that the energy delivered is much larger than the energy for producing a collector no matter the configuration of the collector, and that would probably also be the result with other sources of data and other Boundary conditions.

As the result of the LCA is dependent on many assumptions and delimitations it cannot be completely valid. The aluminium absorber together with an argon filling is, for example, not completely comparable with a copper absorber together with a xenon filling since the conditions for the energy demand for the material and gas extraction can vary depending on local variations of supply. However, the result can be taken as a guideline for reducing the energy demand, even if it cannot be completely accurate under all conditions.

5.3 Suggestions for future work

Some further refinements of the research area of gas-filled solar collectors may still be examined. The suggestions for the future are possible division into several sub divisions which are presented in the following.

5.3.1 Other designs

Some changes in the design would be so large compared to this work that new models would need to be set up. For example these could be:

- Large changes of dimensions - is it, for example, possible to build a 10 m^2 gas-filled, concentrating collector?
- Other materials - is it possible to build a gas-filled polymer collector or all aluminium arbsorbers?
- Collector principles - e.g. can gas pressure be reduced in the cavity (maybe combined with the use of aerogel) or are there other suitable/better tube configurations?

5.3.2 Refinements

The research carried out in this work can be refined in the following ways:

- More detailed study can be made of connections between absorber and glass.
- The mechanical behaviour can be studied when the bends are included in the meander of the tubes in the model.
- Stresses due to different thermal expansion in glass, copper and aluminium can be taken into account.
- Annual performance simulation for a complete solar system.
- A CFD calculation can be made of the gas in the cavity.

6. CONCLUSIONS

The more important conclusions of this work are presented here.

6.1 Configuration

The appropriate collector configuration depends on the criteria selected when the solar collector is to be designed.

Maximum annual yield: If only maximum yield is of interest, use a xenon filling as a first choice and krypton as a second choice together with a normal thick absorber. Absorber material is less important, since it is possible to achieve the same thermal performance with both aluminium and copper.

Maximum net yield during the lifetime: If attention is also paid to the energy demand of production of included components and materials, use a krypton gas filling as a first choice and a normal thick copper absorber. As an alternative, xenon can be used if the collector is designed to work for more than 20 years. An aluminium absorber may also be an alternative; it takes slightly more energy to produce it, but the difference is small.

High yield, low production cost: If value for money is also of interest, the collectors with aluminium absorbers are all better value for money.

High value for money: If it is acceptable to have less than the absolute maximum yield but good value for money, then the collector with the thin aluminium absorber together with krypton or argon is an alternative. Compared with reference 2 (the air filled collector), all noble gas filled collectors examined have higher performance, and most of them are also cheaper.

Minimum cost: If the aim is the lowest possible production cost, then the collectors with a 0.5 mm aluminium absorber should be chosen, together with an argon filling.

It should further be noted that an argon filled collector together with a normal to thick aluminium absorber (e.g. “Ar,Al0.75”) shall not be chosen due to the unsatisfactory factor of safety (see 4.2.3).

6.2 Construction

The optimal use of gas was compiled (see Table 4.2 on page 47) and it could be seen that the most efficient gas volumes are quite modest: 3.9 nl/m^2 for xenon, 5.7 nl/m^2 for krypton, and 8.6 nl/m^2 for argon, (where nl = normal litre at 25 °C gas temperature). These figures also depend on the design temperature of the collector. For further information see Vestlund et al. (2011b).

The factor of safety also needs to be checked. Some general advice for a gas-filled collector is that it is advantageous to have large areas, long tubes and short distances between the absorber and cover glass. The latter distance is, however, more or less fixed by the chosen gas. There are also many other factors to take into account, for example, wind and snow loads, and the formation of the connection between absorber and glass. There should also be free space under the absorber; if the absorber touches the insulation there will be other forces that are not included in the calculations in this project. And there is no point in increasing all thicknesses, because then the factor of safety can decrease.

After the first practical tests have been carried out, the result must be analysed and a great deal of knowledge is needed to be able to understand the results. Calculations can a serve as a guideline for what to do and what not to do. However, practical considerations need to be taken into account and the prototypes will give more knowledge in addition to that given by the calculations.

6.3 Achievements

Sealing and gas filling mean that the gas-filled solar collector is slightly more complex than an open, air filled solar collector. As this solar collector is more effective with the same use of material, it is possible either to improve the performance for the same material cost or to decrease the material cost of the collector and retain the performance.

The sealing also has some advantageous side effects: there cannot be any dust or humidity in a sealed collector. This increases the chances of maintaining performance.

The gas-filled collectors can offer more attractive performance and/or price: It is the manufacturer who must decide whether the technique of gas-filled flat plate solar collectors shall be used to achieve better performance or better assembly prices, or a mixture. The gas-filled collectors are capable of fulfilling both these criteria.

Nomenclature

Symbol	Explanation
A	Area; depending on context: Aperture, cross section or wall area [m^2]
a	Loss coefficient when mean temperature of heat transfer medium is the same as the ambient temperature [W/m^2, K]
b	Temperature dependant loss coefficient [$W/(m^2, K^2)$]
b_0	Incident angle modifier coefficient [-]
d_p	Absorber thickness
d_{pc}	Distance between absorber and glass
d_{tt}	Tube to tube distance
E	Matrix consisting of all heat transfer relationships.
E	Elasticity modulus [N/m^2, Pa]
$e_{1,2}$	Heat transfer element between node 1 and 2 [W/K]
F	Force [N]
F’	Fin efficiency [-]
g	Gravitational constant [9.81 m/s^2]
$G_{Absorbed}$	Absorbed irradiance [W/m^2]
$G_{Incident}$	Incident irradiance [W/m^2]
$G_{t,c}$	Irradiance transmitted through the cover glass [W/m^2]
Gr	Grashof number [-]
J	Jacobian matrix which describes how the different heat transfer sums change as the temperatures changes.
k	Thermal conductivity; material constant [$W/(m^2$,K]
$K_{\tau\alpha}$	Incident angle modifier [-]
L	Plate spacing [m]
L_0	Length from the beginning [m]
n	Amount of gas [moles]
n	Iteration number subscript [-]
n+1	Subscript referring to next iteration [-]
Nu	Nusselts number [-]

Symbol	Explanation
p	Absolute pressure [Pa]
Pr	Prandtl number [-]
q	Usable power [W]
q_c	Power of thermal transfer due to convection [W]
q_k	Power of thermal transfer due to conductance [W]
q_{Loss}	Loss power [W]
$q_{1,2}$	Heat transfer power from node 1 to 2 [W]
$\vec{q}$	Vector with the heat transfer sum at each node in the model; will be $\vec{0}$ when all temperatures are found.
R	Gas konstant [8.314472 $J \cdot K^{-1} \cdot mol^{-1}$]
Ra	Rayleigh number [-]
S	Shape factor [m]
T	Temperature [K or °C]
T_a	Ambient temperature [°C])
T_p	Mean temperature of absorber plate [°C]
T_w	Mean temperature of heat transfer medium [°C]
T_1	Temperature at node 1 [K]
T_2	Temperature at node 2 [K]
$\vec{T}$	Vector with temperatures of all nodes in the model.
$\overrightarrow{t_n}$	Vector giving the temperature change for next attempt.
U_l	Heat loss coefficient referred to mean plate temperature [W/(K,m^2)]
U_o	Heat loss coefficient referred to fluid temperature [W/(K,m^2)
V	Volume [m^3]
x	Thickness of a wall [m]
x	Coordinate in the absorber plane perpendicular to the tubes
y	Coordinate in the absorber plane parallel to the tubes
z	Coordinate perpendicular to the absorber plane

Symbol	Explanation
α	Absorptance; fraction of the incident radiation that is absorbed by the surface [-]
β	Slope [rad or °]
β'	Volumetric constant of expansion, based on the mean temperature in the medium ($\beta' = 1/T$) [K^{-1}]
ΔT	Temperature difference in general or difference between mean heat transfer media temperature and ambient temperature [K]
ΔT_{local}	Difference between each local point on fin and tube respectively and ambient temperature [K]
δ	Elongation [m]
ε	Strain [-]
η	Efficiency [-]
η_0	Efficiency when mean temperature of heat transfer media is the same as the ambient [-].
θ	Angle between surface normal and incident radiation [rad or °]
ν	Kinematic viscosity [m^2/s]
ρ	Density [kg/m^3]
σ	Stress or normal stress depending on context [N/m^2]
σ_e	Endurance; limit of the amount of periodical stress a material can withstand repeatedly - number of times (typically 10^7 times) [N/m^2]
σ_{UTC}	Ultimate strength: limit of how much stress the material can withstand when it is loaded once [N/m^2]
τ	Transmittance; ratio of the light penetrating the glass to the total amount of light incident on it [-]
τ	Shear stress [Pa].
$(\tau\alpha)$	optical efficiency at a given incident angle [-]
$(\tau\alpha)_n$	optical efficiency perpendicular to the collector [-]
+ exponent	Only positive values of the terms in the square brackets are to be used.

References

Air-Liquide, 2006. Physical data of gasses. http://www.airliquide.com/.

Alvarez, H., 1990. Energiteknik (Energy Technology), ISBN: 91-44-31471-X, Studentlitteratur, Lund, Sweden, 1294p.

Baumann, H. and Cowell, S. J., 1999. An evaluative framework for conceptual and analytical approaches used in environmental management. Greener Management International(26): 109-122.

Baumann, H. and Tillman, A.-M., 2004. The Hich Hiker's Guide to LCA An orientation in life cycle assessment methodology and application, ISBN: 91-44-02364-2, Studentlitteratur Lund, Lund, 543 p.

Berg, O. and Burvall, J., 1998. Kreativ problemlösning (Creative problem solutions), ISBN: 91-7548-506-0, Industrilitteratur AB, Arlöv, 170p.

Buderus, 2005. Katalog Heiztechnik 2005/1 – Teil 1, BBT Thermotechnik GmbH. 2005: p10016-10018, (70p).

Cooper, P. I. and Dunkle, R. V., 1981. A non-linear flat-plate collector model. Solar Energy 26(2): 133-140.

Duffie, J. A. and Beckman, W. A., 2006. Solar engineering of thermal processes, ISBN: 13 978-0-471-69867-8, John Wiley & Sons, Inc., Hoboken, New Jersey, 908 p.

Edlund, L., 2010. Personal communication about price of argon gas, AGA AB

Eisenmann, W., 2002. Untersuchungen zu Leistungsfähigkeit und Materialaufwand von Sonnenkollektoren mit serpentinenund harfenartiger Rohrverlegung. Fachbereich Physik Marburg, der Philipps-Universität Doktorgrades der Naturwissenschaften (Dr. rer. nat.): pp 149.

Eisenmann, W., Vajen, K. and Ackermann, H., 2004. On the correlations between collector efficiency factor and material content of parallel flow flat-plate solar collectors. Solar Energy 76(4): p 381.

EISherbiny, S. M., Raithby, G. D. and Hollands, K. G. T., 1982. Heat transfer by natural convection across vertical and inclined air layers. The ASME Journal of Heat Transfer 104(1)(February): 96-102.

Hammond, G. P., 2004. Towards sustainability: energy efficiency, thermodynamic analysis, and the 'two cultures'. Energy Policy 32(16): 1789–1798.

Hollands, K. G. T., Unni, T. E., Raithby, G. D. and Konicek, L., 1976. Free convective heat transfer across incllined air layers. The ASME Journal of Heat Transfer 98 Ser C(2): 189-193.

Holman, J. P., 2002. Heat Transfer, ISBN: 0-07-240655-0, McGraw-Hill College, Boston, USA, 665p.

Konttinen, P., 2007. Communication about commonly used flat plate solar collector absorber thicknesses. Beijing, China, Outokumpu Copper

Lide, D. R., 1994. CRC Handbook of chemistry and physics : a ready-reference book of chemical and physical data, ISBN: 0-8493-0596-9, CRC Press, Boca Raton.

Lund, H., 2005. Grundläggande hållfasthetslära (The basics of mechanics of materials), ISBN: 91-972860-2-8, Fingraf Tryckeri AB, Södertälje, 393p.

Norgate, T. E., Jahanshahi, S. and Rankin, W. J., 2006. Assessing the environmental impact of metal production processes. Journal of Cleaner Production 15(8-9): 838 - 848.

Öko-Institut (Institut für angewandte Ökologie), 2010. Global emission model for integrated systems (GEMIS), German environmental database. version 4.6

Olofsson, M., 2010. Personal communication about price of window framings. Borlänge, Haglöfs glas AB

Pettersson, B., 2005. Personal communication about prices of xenon and krypton, Aga Gas

Pohl, P., 1999. Numeriska metoder, NADA, KTH, Stockholm.

Qaist, 2010. Evaluation energy output v2.1 - general version - unlocked - March 2010.xls. V. 2008-11-27.

Quicklund, H. and Johansson, G., 2004. Rapport Energideklaration för solfångare med AR-glas (Report energy declaration for solar collector with AR-glass). Borås, SP Sveriges Provnings och Forskningsinstitut AB (SP Technical Research Institute of Sweden): 5p.

Skandinaviska Enskilda Banken AB, 2009. Commodity market prices, accessed 2009.12.16. http://www.seb.se/.

Solentek AB, 2010. Personal communication about prices of insulation, glass, back and frame for solar collectors. Djurmo

Souka, A. F. and Safwat, H. H., 1966. Determination of the optimum orientations for the double-exposure, flat-plate collector and its reflectors. Solar Energy 10(4): 170-174.

SP Technical Research Institute of Sweden, 2010. Förteckning över solfångare godkända för Boverkets installationsstöd, accessed 2010.03.31 (List of solar collectors approved for installation subsidy in Sweden) Borås

Sunnersjö, S., 1992. FEM i praktiken (FEM in practice), ISBN: 91-7548-541-9, Industrilitteratur AB, Uddevalla, 250p.

Vedung, E., 1998. Utvärdering i politik och förvaltning (Evaluation in politics and administration), ISBN: 91-44-34262-4, Studentlitteratur, Lund, 260 p.

Vestlund, J., Dalenbäck, J.-O. and Rönnelid, M., 2011a. Mechanical Performance of sealed solar collectors. Sol. Energy (2011), doi:10.1016/j.solener.2011.10.005, Elsevier

Vestlund, J., Dalenbäck, J.-O. and Rönnelid, M., 2011b. Thermal and mechanical performance of sealed, gas-filled, flat plate solar collectors. Sol. Energy (2011), doi:10.1016/j.solener.2011.08.023, Elsevier

Vestlund, J., Rönnelid, M. and Dalenbäck, J.-O., 2009. Thermal performance of gas-filled flat plate solar collectors. Solar Energy 83(6): 896-904.

Wahlström, L., 2011. Personal communication about thicknesses of aluminium absorbers. Finspång, S-Solar

Weir, G. and Muneer, T., 1998. Energy and environmental impact analysis of double-glazed windows. Energy Convers. Mgmt 39(3/4): pp 243-256.